# Calorimetry at LHC

Arno Straessner
TU Dresden

Graduiertenkolleg “Masse, Spektrum, Symmetrie”
DESY Zeuthen
October 4-8, 2011

# Outline

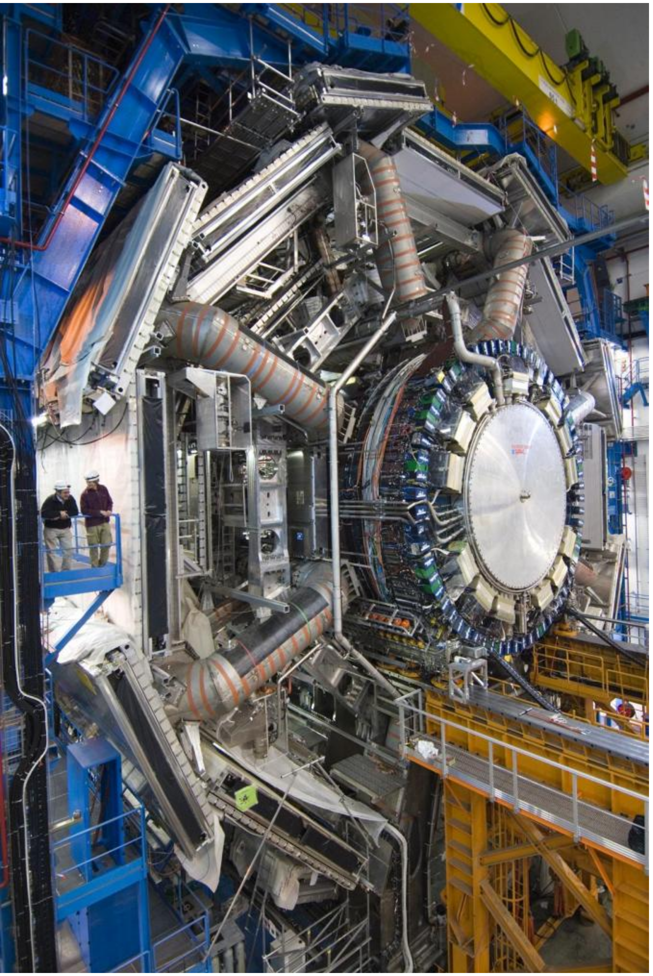

- Physics of calorimeters
  → tutorial session on simulation of calorimeters with Geant4
- Calorimeters at LHC – examples
- Calorimeters for the High Luminosity LHC

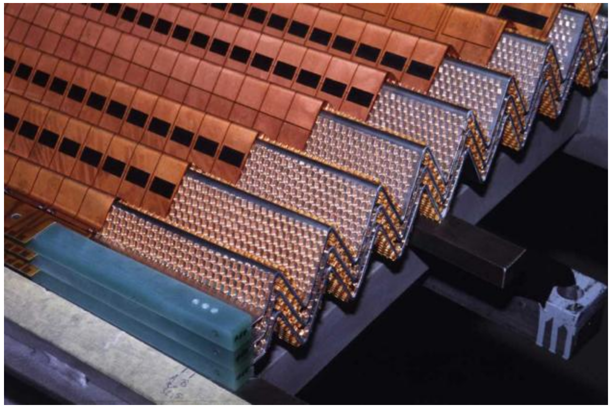

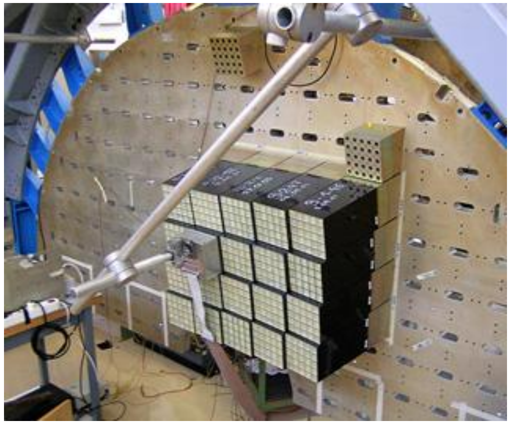

# Physics of Calorimeters

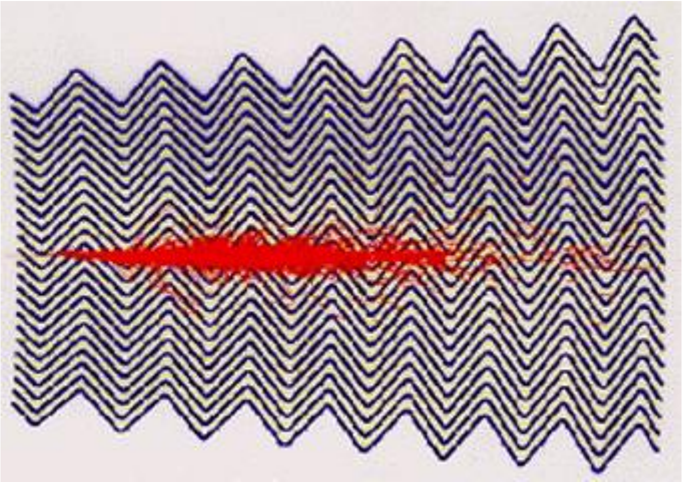

# Basic Functionality

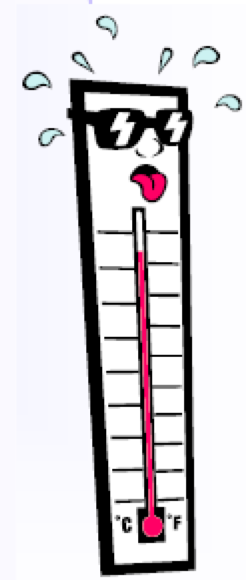

- Basic mechanism for calorimetry in paricle physics: formation of
  - ⇨ electromagnetic
  - ⇨ or hadronic showers.

- Finally, the energy is converted into ionization or excitation of the matter.

  Charge

  Scintillation light

  Cerenkov light

- Calorimetry is a “destructive” method. The energy and the particle get absorbed!

- Detector response $\propto$ E

- Calorimetry works both for
  - ⇨ charged ($e^{\pm}$ and hadrons) → Complementary information to p-measurement
  - ⇨ and neutral particles ($n,\gamma$) → Only way to get direct kinematical information for neutral particles

# Resolution of Tracking Detectors and Calorimeters

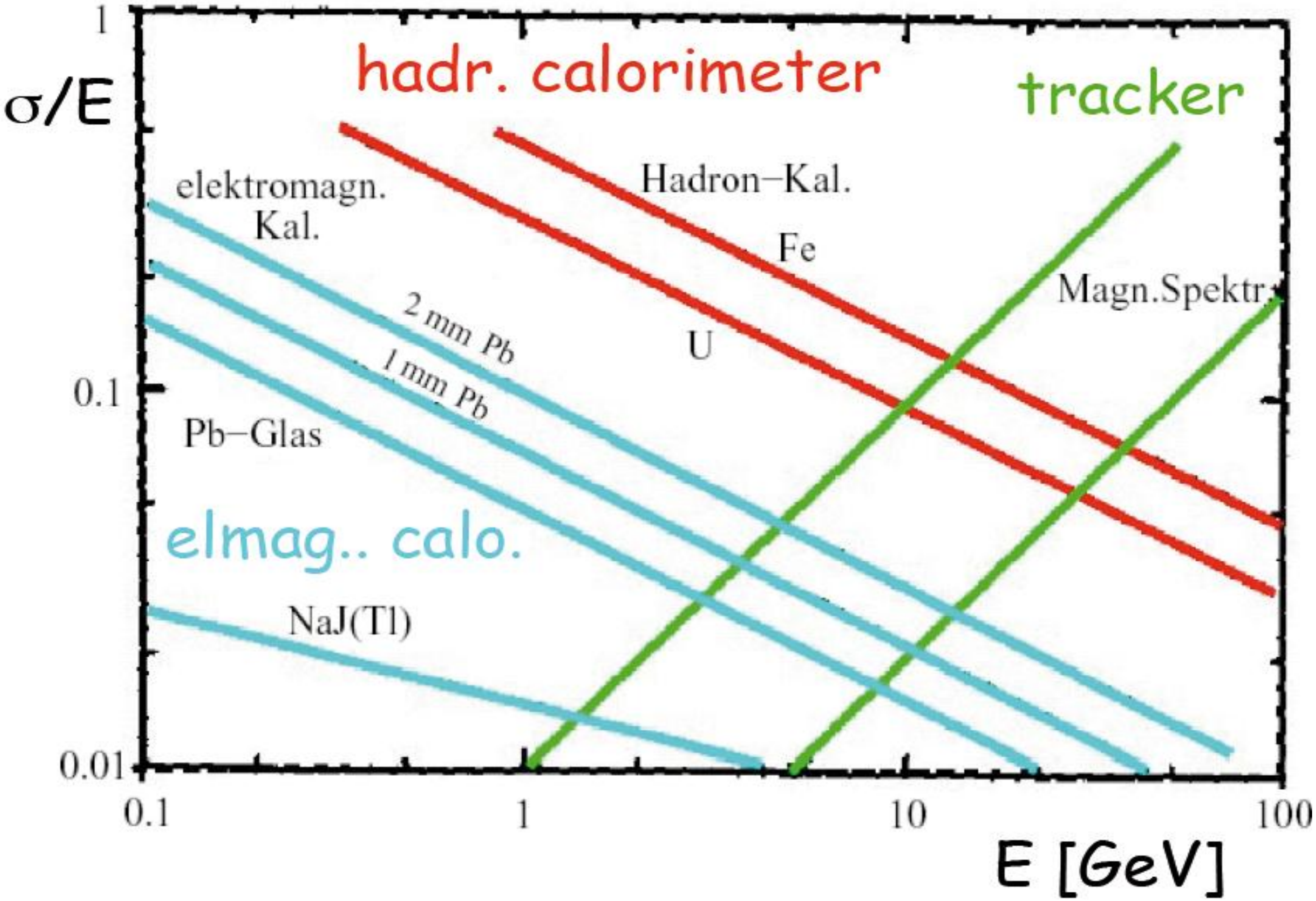


$$\text{For tracker: track curvature} \propto p_T \rightarrow \frac{\sigma(p_T)}{p_T} \propto p_T$$

$$\text{For calorimeters: number of energy deposits} \propto E \rightarrow \frac{\sigma(E)}{E} \propto \frac{\sqrt{N}}{N} \propto \frac{\sqrt{E}}{E} \propto \frac{1}{\sqrt{E}}$$

# Electromagnetic Cascades

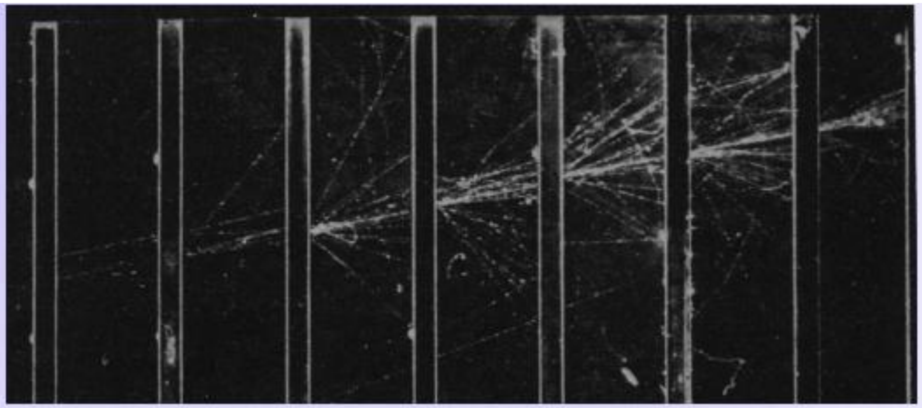

Electron shower in a cloud chamber with lead absorbers

## Simple qualitative model

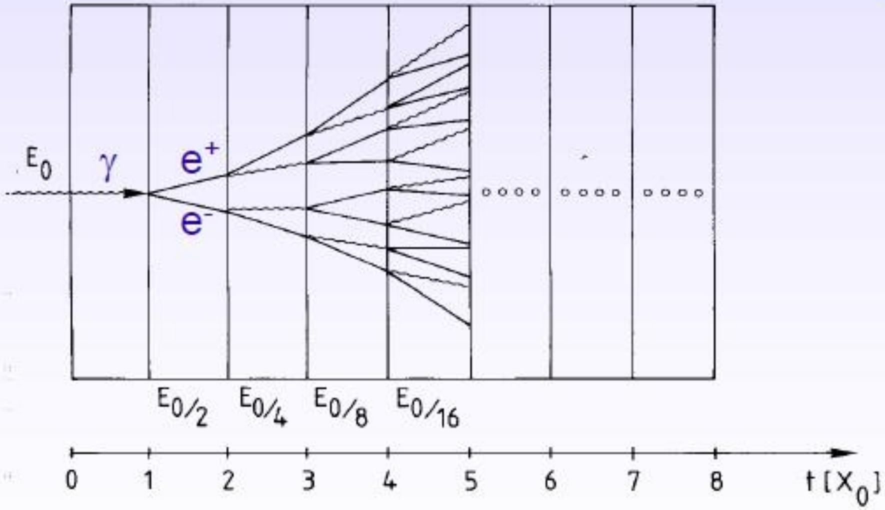


- Consider only Bremsstrahlung and (symmetric) pair production.
- Assume: $X_0 \sim \lambda_{pair}$

$$N(t) = 2^t \qquad E(t)/\,particle = E_0 \cdot 2^{-t}$$

Process continues until $E(t) < E_c$

$$N^{total} = \sum_{t=0}^{t_{\max}} 2^t = 2^{(t_{\max}+1)} - 1 \approx 2 \cdot 2^{t_{\max}} = 2\frac{E_0}{E_c}$$

$$t_{\max} = \frac{\ln E_0 / E_c}{\ln 2}$$

After $t = t_{max}$ the dominating processes are ionization, Compton effect and photo effect → absorption of energy.

CERN Academic Training Programme 2004/2005

- longitudinal profile: $$\frac{dE}{dt} \propto t^{\alpha} e^{-t}$$

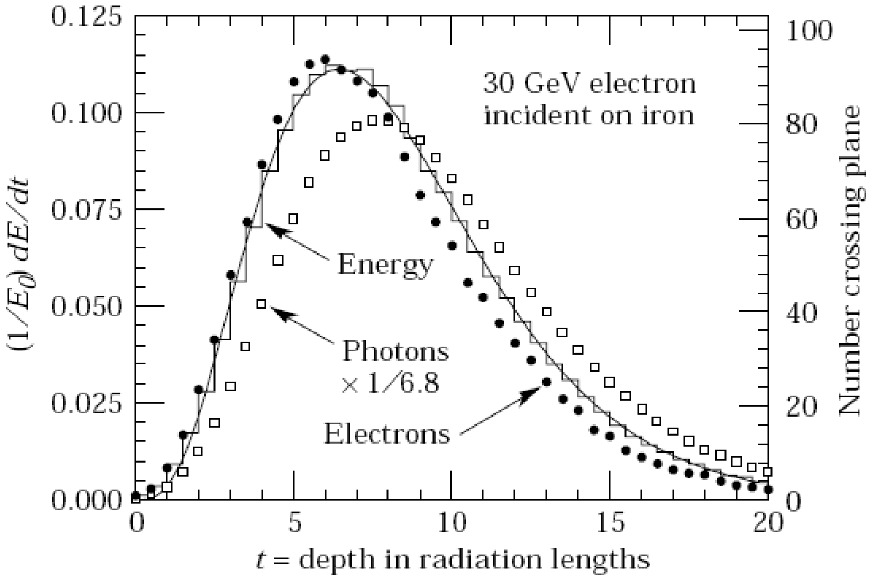


- maximum and 95% containment:

$$t_{\max} = \ln \frac{E_0}{E_c} \frac{1}{\ln 2}$$

$$t_{95\%} \approx t_{\max} + 0.08Z + 9.6$$

- $E_c$ = energy at which ionisation and bremsstrahlung have the same dE/dx
  ~ energy at which dE/dx per $X_0$ by ioniation is equal to E

→ when you simulate e.m. showers, a low energy cut-off can be used
→ different “range” for particle showers in different materials

# Electromagnetic Cascades – Shower Profiles

- longitudinal profile:

$$\frac{dE}{dt} \propto t^{\alpha} e^{-t}$$

- maximum and 95% containment:

$$t_{\max} = \ln \frac{E_0}{E_c} \frac{1}{\ln 2}$$

$$t_{95\%} \approx t_{\max} + 0.08Z + 9.6$$

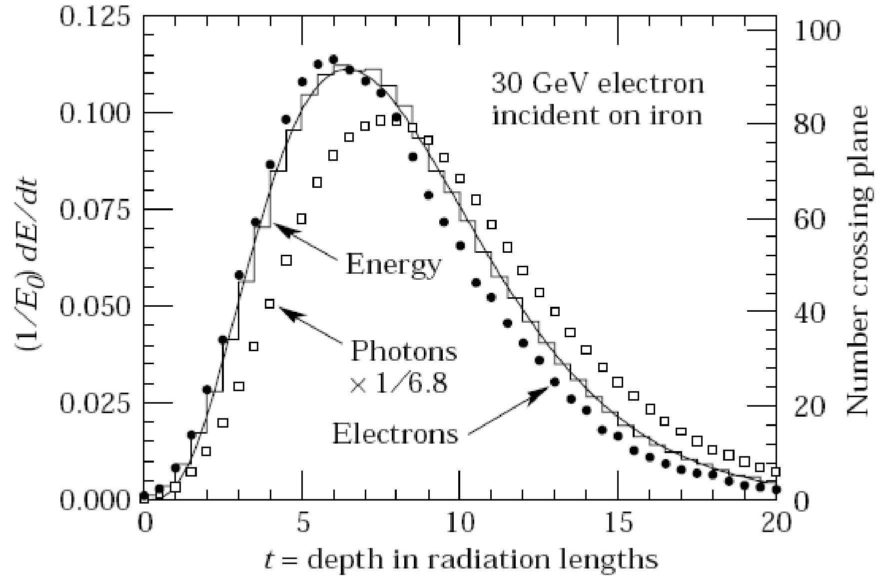


- $E_c$ = energy at which ionisation and bremsstrahlung have the same dE/dx
  ~ energy at which dE/dx per $X_0$ by ioniation is equal to E
- transverse profile given by Moliere radius: $\mathbf{R_M = 7g\ cm^{-2}\ A/Z}$
  - $\mathbf{R(90\%) \approx 1\ R_M}$
  - $\mathbf{R(95\%) \approx 2\ R_M}$
  - $\mathbf{R(99\%) \approx 3.5\ R_M}$

1 GeV e⁻ in lead

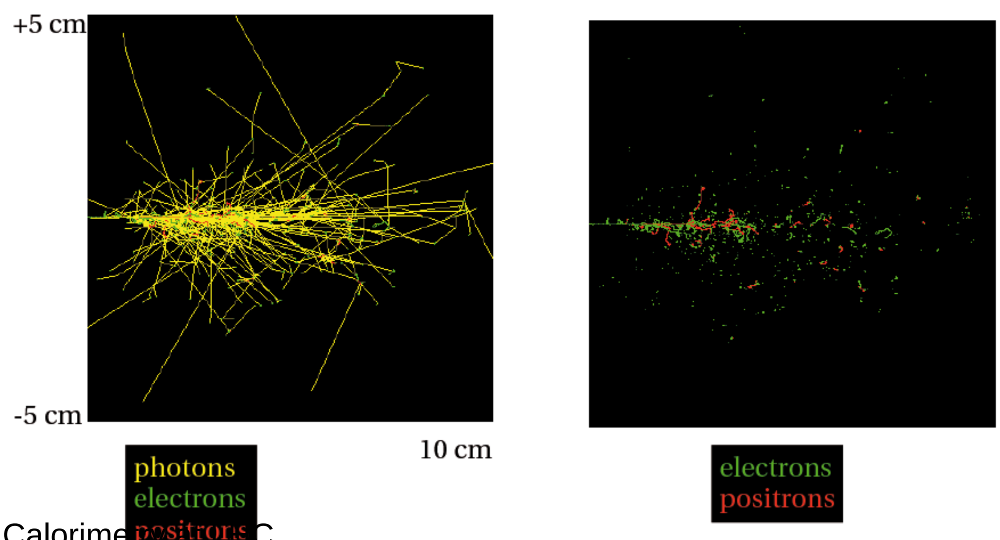


- exponential decrease of particle density at shower boundary → mainly photons

# Detector Active Material

energy measurement by:

- scintillation light:
  - crystals: NaI(Tl), CsI(Tl), CsI, BaF2, BGO, PbWO4
  - good energy resolution
  - problem: not fast response
  - example: CMS (PbWO4), Babar (CsI(Tl)), Belle (CsI(Tl)), L3(BGO)

- Cherenkov effect:
  - higher energy threshold (7 MeV), less photons
  - fast
  - example: Jade (lead glass), OPAL (lead glass)

- ionisation + charge measurement:
  - liquid argon, liquid krypton → sampling calorimeters
  - example: ATLAS(LAr), H1(LAr), NA48(LKr)

# Resolution of EM Calorimeters

In general the energy resolution of a calorimeter can be parametrised as:

$$\frac{\sigma(E)}{E} = \frac{a}{\sqrt{E}} \oplus b \oplus \frac{c}{E}$$

**Stochastic Term**

- stochastic fluctuations in shower development
- sampling fluctuations in case of sampling calori-meter
- photo-electron statistics
  → Poisson distribution
  $\sigma \sim 1/\sqrt{N} \sim 1/\sqrt{E}$

**Constant Term**

- inhomogeneities dead material
- non-linearities
- leakage
  →Presampler/Tailcatcher
- inter-calibration between individual cells

$\sigma(E)/E = b$

**Noise Term**

$\sigma(E) = c \Rightarrow \sigma(E)/E = c/E$

- electronic noise
- radioactivity
- pile-up

# Sampling Calorimeters

$$N^{total} \propto \frac{E_0}{E_c}$$ total number of track segments

$$T \propto \frac{E_0}{E_c} X_0$$ total track length

d = absorber thickness per layer

$N_{\text{track-segments}} = T / d = (E/E_c)\ (X_0 / d)$

$$\boldsymbol{\sigma(E)/E \sim \sqrt{N}/N \sim \sqrt{(E_c/E)}\ \sqrt{(d/X_0)}}$$

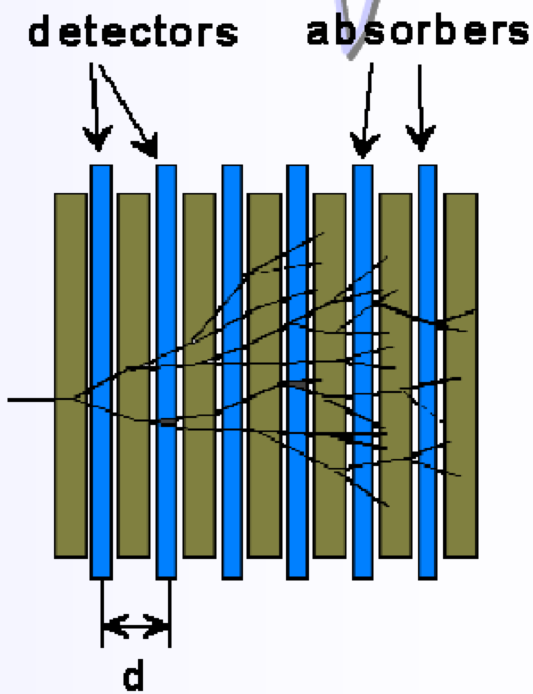


## Pathlength fluctuations + Landau fluctuations

wide spread angular distribution of (low energy) $e^{\pm}$

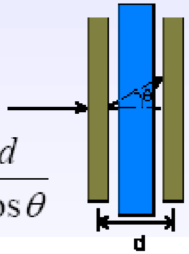


$$d_{eff} = \frac{d}{\cos\theta}$$

In thin gas detector layers the deposited energy shows typical Landau tails

(C. Fabjan, T. Ludlam, CERN-EP/82-37)

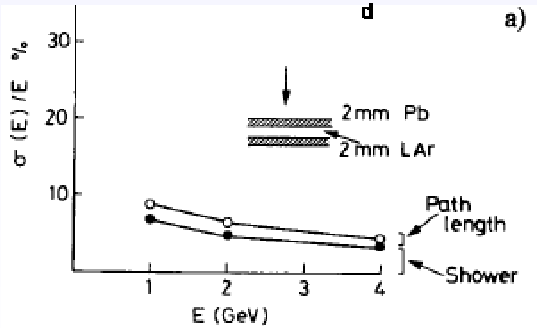


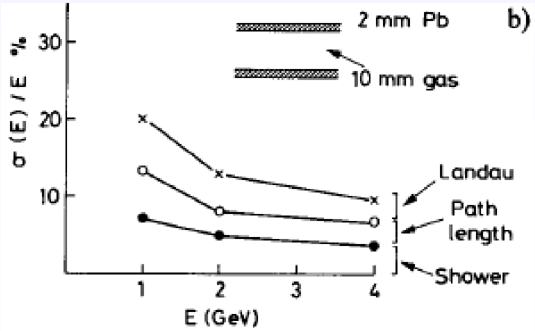

**Table 28.9:** Resolution of typical electromagnetic calorimeters. $E$ is in GeV.

| Technology (Exp.) | Depth | Energy resolution | Date |
|---|---|---|---|
| NaI(Tl) (Crystal Ball) | $20X_0$ | $2.7\%/\mathrm{E}^{1/4}$ | 1983 |
| $Bi_4Ge_3O_{12}$ (BGO) (L3) | $22X_0$ | $2\%/\sqrt{E} \oplus 0.7\%$ | 1993 |
| CsI (KTeV) | $27X_0$ | $2\%/\sqrt{E} \oplus 0.45\%$ | 1996 |
| CsI(Tl) (BaBar) | $16$–$18X_0$ | $2.3\%/E^{1/4} \oplus 1.4\%$ | 1999 |
| CsI(Tl) (BELLE) | $16X_0$ | $1.7\%$ for $E_\gamma > 3.5$ GeV | 1998 |
| $PbWO_4$ (PWO) (CMS) | $25X_0$ | $3\%/\sqrt{E} \oplus 0.5\% \oplus 0.2/E$ | 1997 |
| Lead glass (OPAL) | $20.5X_0$ | $5\%/\sqrt{E}$ | 1990 |
| Liquid Kr (NA48) | $27X_0$ | $3.2/\%\sqrt{E} \oplus 0.42\% \oplus 0.09/E$ | 1998 |
| Scintillator/depleted U (ZEUS) | $20$–$30X_0$ | $18\%/\sqrt{E}$ | 1988 |
| Scintillator/Pb (CDF) | $18X_0$ | $13.5\%/\sqrt{E}$ | 1988 |
| Scintillator fiber/Pb spaghetti (KLOE) | $15X_0$ | $5.7\%/\sqrt{E} \oplus 0.6\%$ | 1995 |
| Liquid Ar/Pb (NA31) | $27X_0$ | $7.5\%/\sqrt{E} \oplus 0.5\% \oplus 0.1/E$ | 1988 |
| Liquid Ar/Pb (SLD) | $21X_0$ | $8\%/\sqrt{E}$ | 1993 |
| Liquid Ar/Pb (H1) | $20$–$30X_0$ | $12\%/\sqrt{E} \oplus 1\%$ | 1998 |
| Liquid Ar/depl. U (DØ) | $20.5X_0$ | $16\%/\sqrt{E} \oplus 0.3\% \oplus 0.3/E$ | 1993 |
| Liquid Ar/Pb accordion (ATLAS) | $25X_0$ | $10\%/\sqrt{E} \oplus 0.4\% \oplus 0.3/E$ | 1996 |

homogeneous

sampling

Various processes involved.
Much more complex than
electromagnetic cascades.

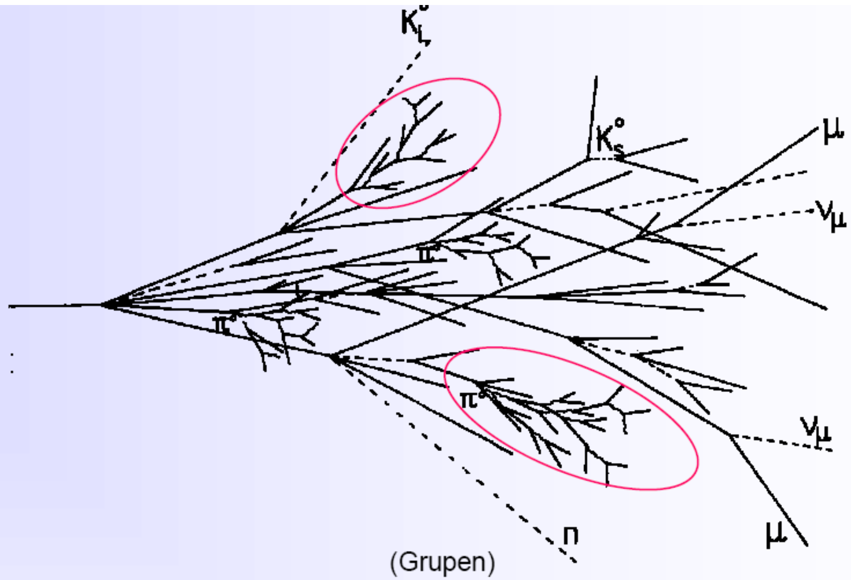

(Grupen)

A hadronic shower contains two components:

**hadronic** + **electromagnetic**

- charged hadrons p,$\pi^{\pm}$,$K^{\pm}$,
- nuclear fragmets ….
- breaking up of nuclei (binding energy)
- neutrons, neutrinos, soft $\gamma$'s, muons

neutral pions $\rightarrow 2\gamma$
$\rightarrow$ electromagnetic cascades

$$\boxed{n(\pi^0) \approx \ln E(GeV) - 4.6}$$

example $E = 100$ GeV: $n(\pi^0) \approx 18$

invisible energy $\rightarrow$ large energy fluctuations $\rightarrow$ limited energy resolution

CERN Academic Training Programme 2004/2005

# Compensation

A hadron calorimeter shows in general different efficiencies for the detection of the hadronic and electromagnetic components $\varepsilon_h$ and $\varepsilon_e$.

$$R_h = \varepsilon_h E_h + \varepsilon_e E_e$$

$\varepsilon_h$: hadron efficiency
$\varepsilon_e$: electron efficiency

The fraction of the energy deposited hadronically depends on the energy (remember n($\pi^0$))

$$\boxed{\frac{E_h}{E} = 1 - f_{\pi^0} = 1 - k \ln E \ \ (GeV) \qquad k \approx 0.1}$$

→ Response of calorimeter to hadron shower becomes non-linear

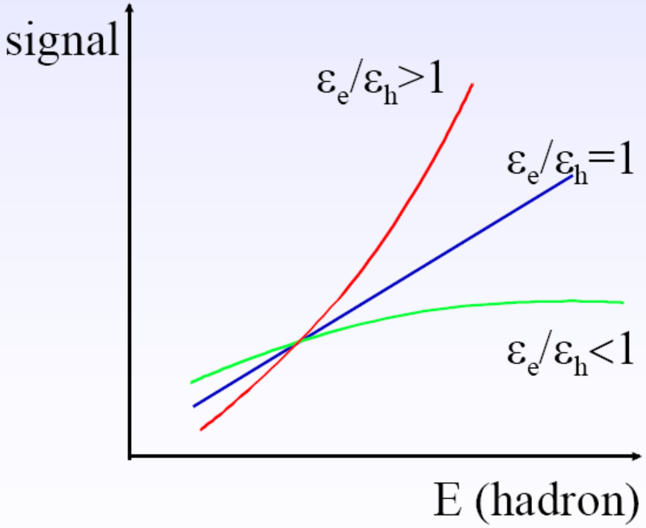


Energy resolution degraded !

$$\boxed{\frac{\sigma(E)}{E} = \frac{a}{\sqrt{E}} + b \cdot \left| \frac{\varepsilon_e}{\varepsilon_h} - 1 \right|}$$

(Schematically after Wigmans R. Wigmans NIM A 259 (1987) 389)

CERN Academic Training Programme 2004/2005

increase $\varepsilon_h$ : use Uranium absorber $\rightarrow$ amplify neutron and soft $\gamma$ component by fission + use hydrogeneous detector $\rightarrow$ high neutron detection efficiency

decrease $\varepsilon_e$ : combine high Z absorber with low Z detectors. Suppressed low energy $\gamma$ detection ($\sigma_{photo} \propto Z^5$)

offline compensation : requires detailed fine segmented shower data $\rightarrow$ event by event correction.

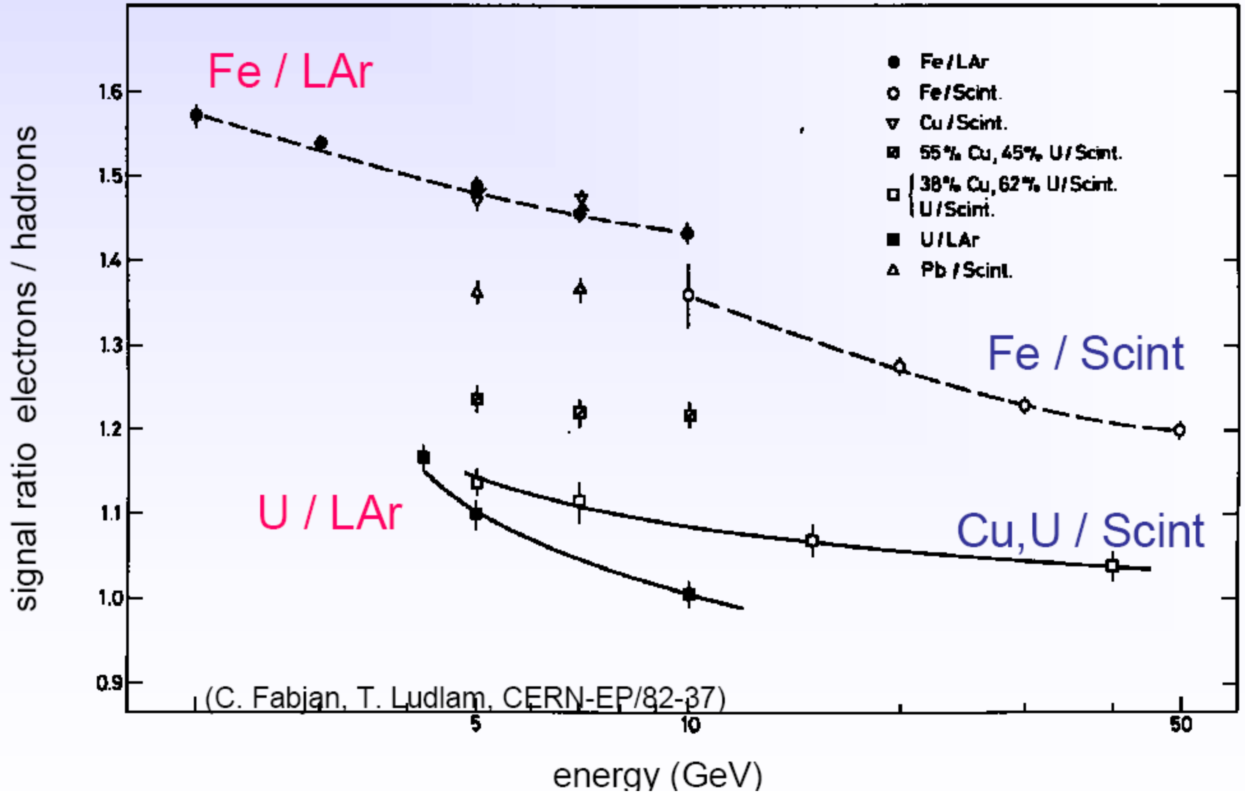

# Calorimeters at LHC
# Examples

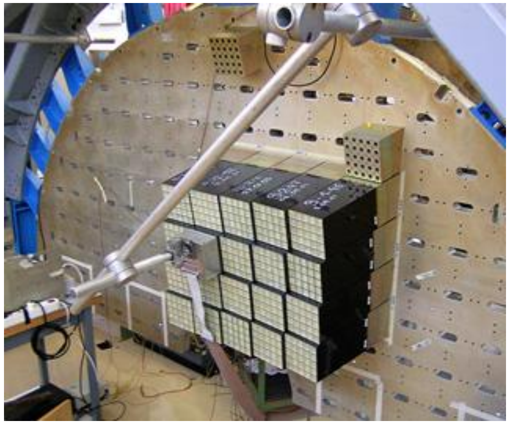

# ATLAS and CMS Electromagnetic Calorimeters

ATLAS

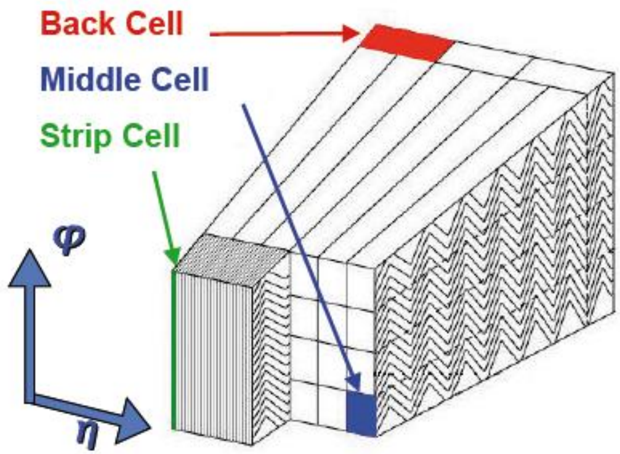


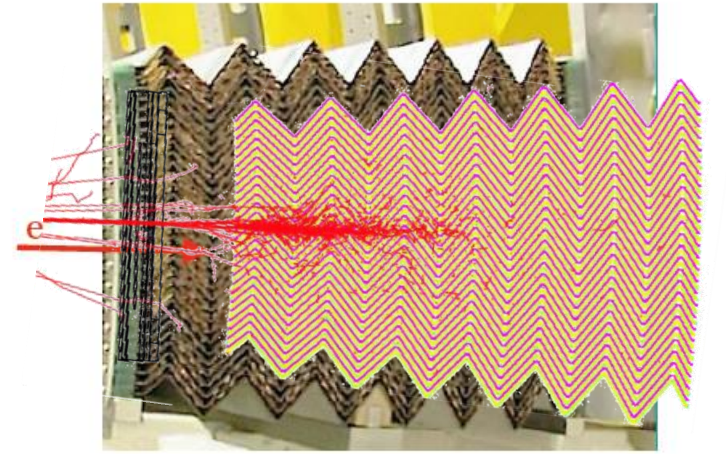


CMS

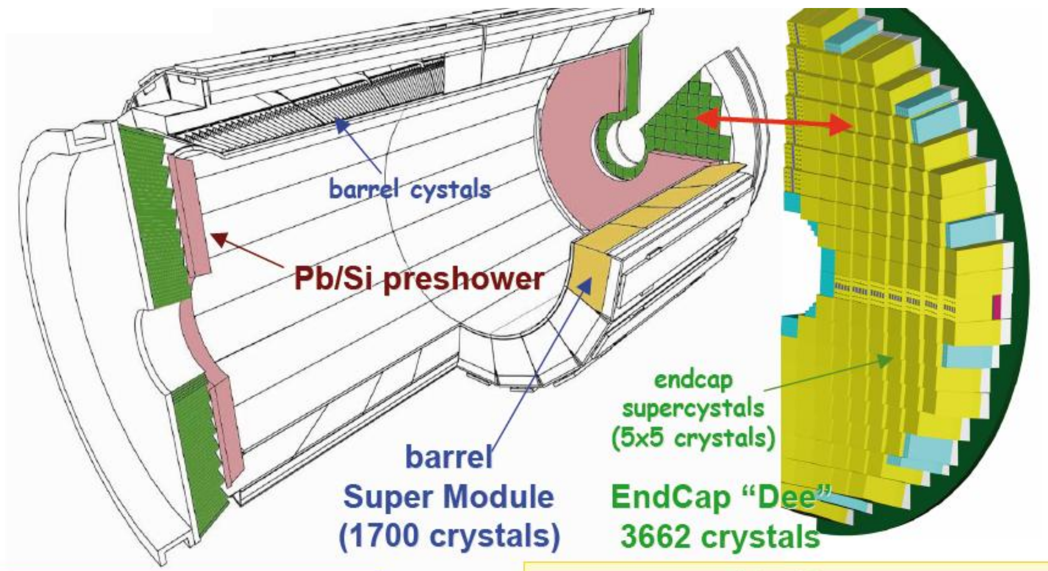


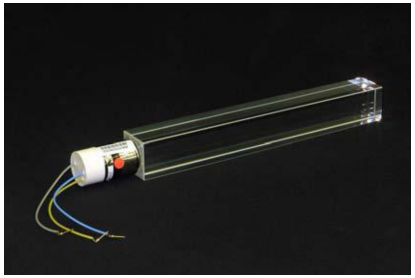

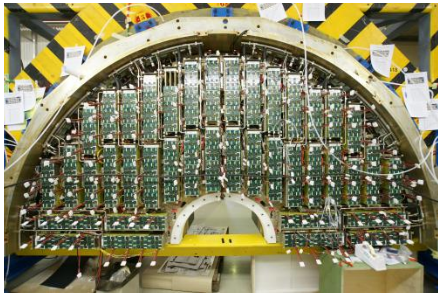

Barrel:
61200 $PbWO_4$ crystals
($2x2x23cm^3$)

EndCaps:
14648 $PbWO_4$ crystals
($3x3x22cm^3$)

# Performance of the ATLAS LAr Calorimeter

- 10 M minimum-bias events
- 130,000 electron candidates

- fraction of energy in the calorimeter layers

- most energy in 1st and 2nd layer
- little energy in 3rd layer
- shower reasonably well contained

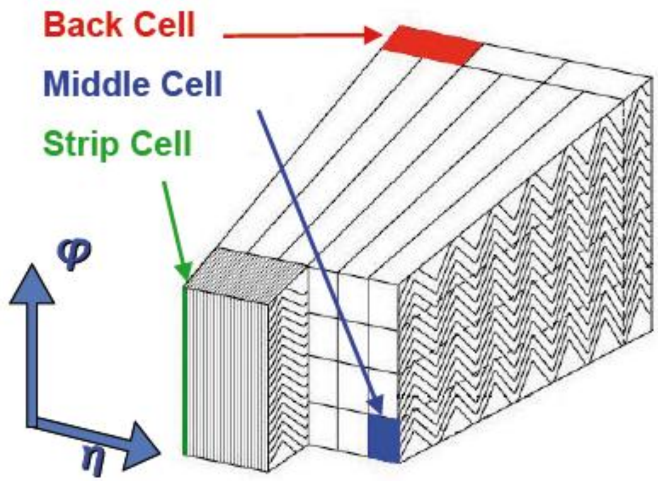


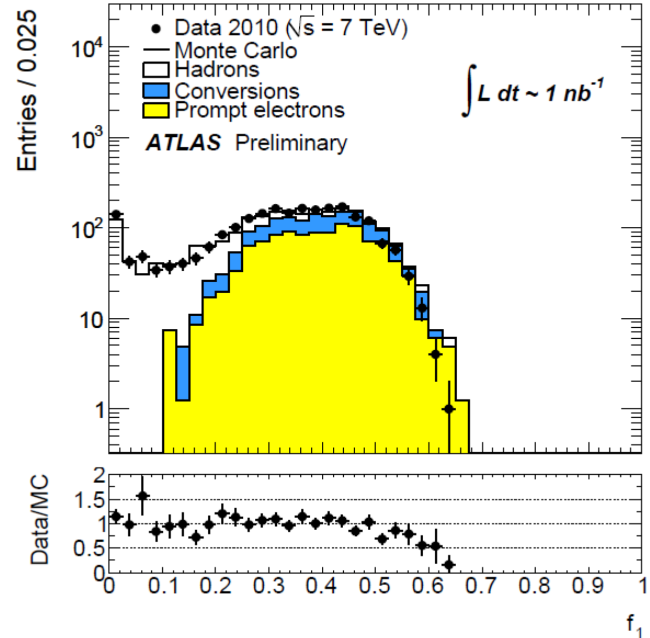


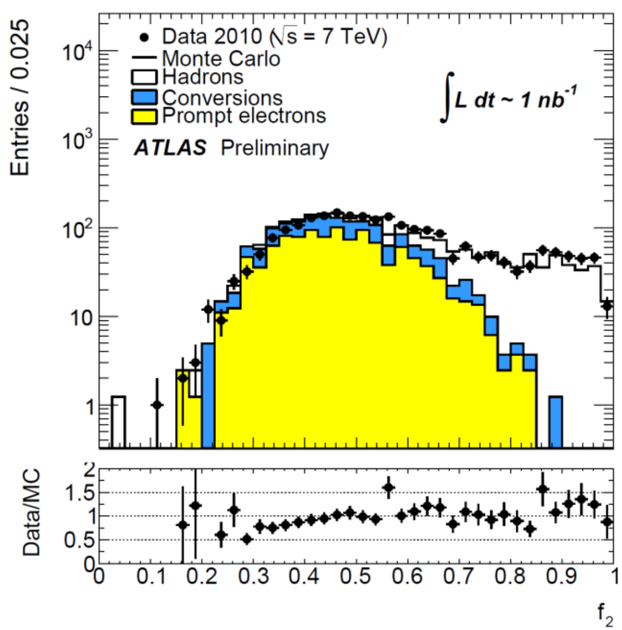


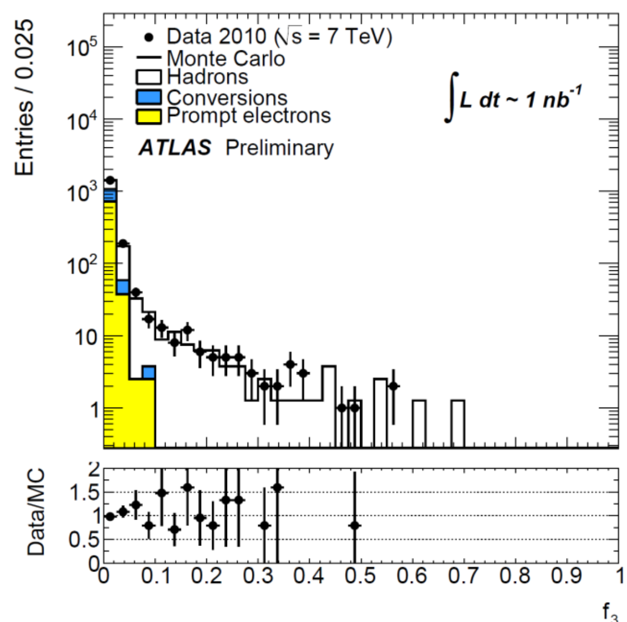


$E_T^{cluster} > 5$ GeV, $E_T^{raw} > 4$ GeV
$|\eta_{s2}| < 2.0$ [exclude $1.37 < |\eta_{s2}| < 1.52$]

+ track & vertex criteria

# ATLAS and CMS Electromagnetic Calorimeters

| | ATLAS | | CMS | |
|---|---|---|---|---|
| Technology | Lead/LAr accordion | | $PbWO_4$ scintillating crystals | |
| Channels | Barrel | End caps | Barrel | End caps |
| | 110,208 | 63,744 | 61,200 | 14,648 |
| Granularity | $\Delta\eta \times \Delta\phi$ | | $\Delta\eta \times \Delta\phi$ | |
| Presampler | $0.025 \times 0.1$ | $0.025 \times 0.1$ | | |
| Strips/ Si-preshower | $0.003 \times 0.1$ | $0.003 \times 0.1$ to $0.006 \times 0.1$ | | $32 \times 32$ Si-strips per 4 crystals |
| Main sampling | $0.025 \times 0.025$ | $0.025 \times 0.025$ | $0.017 \times 0.017$ | $0.018 \times 0.003$ to $0.088 \times 0.015$ |
| Back | $0.05 \times 0.025$ | $0.05 \times 0.025$ | | |
| Depth | Barrel | End caps | Barrel | End caps |
| Presampler (LAr) | 10 mm | $2 \times 2$ mm | | |
| Strips/ Si-preshower | $\approx 4.3\ X_0$ | $\approx 4.0\ X_0$ | | $3\ X_0$ |
| Main sampling | $\approx 16\ X_0$ | $\approx 20\ X_0$ | $26\ X_0$ | $25\ X_0$ |
| Back | $\approx 2\ X_0$ | $\approx 2\ X_0$ | | |
| Noise per cluster | 250 MeV | 250 MeV | 200 MeV | 600 MeV |
| Intrinsic resolution | Barrel | End caps | Barrel | End caps |
| Stochastic term *a* | 10% | 10 to 12% | 3% | 5.5% |
| Local constant term *b* | 0.2% | 0.35% | 0.5% | 0.5% |

# ATLAS and CMS Hadronic Calorimeters

ATLAS

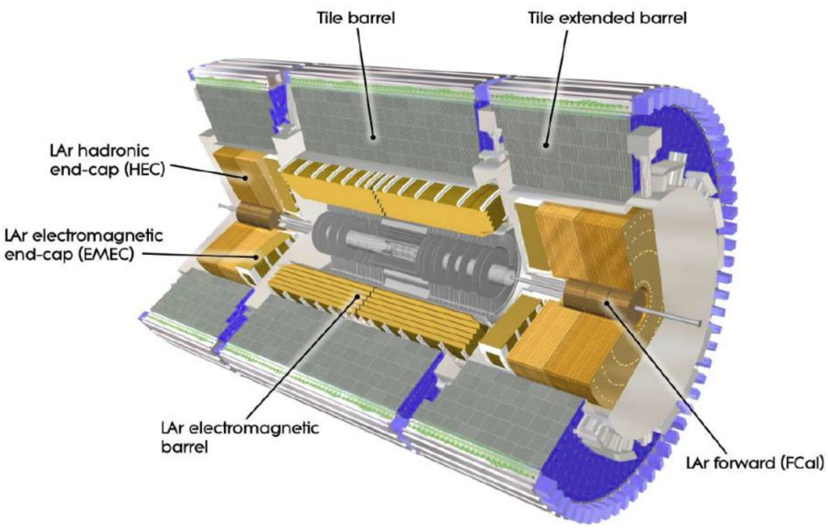


steel + scintillator tiles

optical signals read out with PMTs

CMS


Hybrid Photo Diode

optical signal transmission

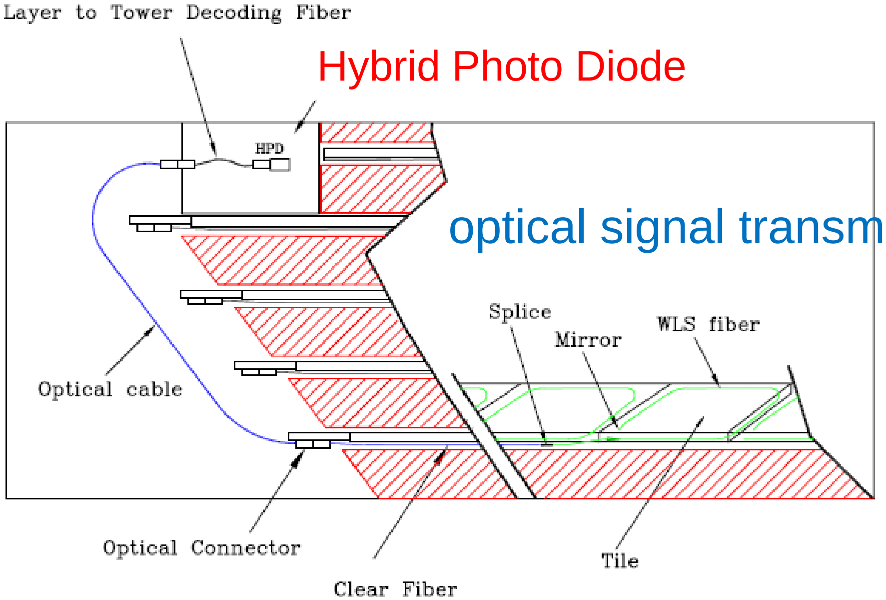


WLS=wavelength-shifting fibre

# ATLAS and CMS Hadronic Calorimeters

| | ATLAS | CMS |
|---|---|---|
| **Technology** | | |
| Barrel/Ext. barrel | 14 mm iron/3 mm scint. | 50 mm brass/3.7 mm scint. |
| End caps | 25–50 mm copper/8.5 mm LAr | 78 mm brass/3.7 mm scint. |
| Forward | Copper (front) - Tungsten (back)/0.25–0.50 mm LAr | Steel/0.6 mm quartz |
| **Channels** | | |
| Barrel/Ext. barrel | 9852 | 2592 |
| End caps | 5632 | 2592 |
| Forward | 3524 | 1728 |
| **Granularity ($\Delta\eta \times \Delta\phi$)** | | |
| Barrel/Ext. barrel | $0.1 \times 0.1$ to $0.2 \times 0.1$ | $0.087 \times 0.087$ |
| End caps | $0.1 \times 0.1$ to $0.2 \times 0.2$ | $0.087 \times 0.087$ to $0.18 \times 0.175$ |
| Forward | $0.2 \times 0.2$ | $0.175 \times 0.175$ |
| **Samplings ($\Delta\eta \times \Delta\phi$)** | | |
| Barrel/Ext. barrel | 3 | 1 |
| End caps | 4 | 2 |
| Forward | 3 | 2 |
| **Abs. lengths (min.-max.)** | | |
| Barrel/Ext. barrel | 9.7–13.0 | 7.2–11.0<br>10–14 (with coil/HO) |
| End caps | 9.7–12.5 | 9.0–10.0 |
| Forward | 9.5–10.5 | 9.8 |

# Hadronic Calorimeter Performance in Testbeams

| | ATLAS | | | | CMS | |
|---|---|---|---|---|---|---|
| | Barrel LAr/Tile | | End-cap LAr | | | |
| | Tile | Combined | HEC | Combined | Had. barrel | Combined |
| Electron/hadron ratio | 1.36 | 1.37 | 1.49 | | | |
| Stochastic term | $45\%/\sqrt{E}$ | $55\%/\sqrt{E}$ | $75\%/\sqrt{E}$ | $85\%/\sqrt{E}$ | $100\%/\sqrt{E}$ | $70\%/\sqrt{E}$ |
| Constant term | 1.3% | 2.3% | 5.8% | $< 1\%$ | | 8.0% |
| Noise | Small | 3.2 GeV | | 1.2 GeV | Small | 1 GeV |

The measured electron/hadron ratios are given separately for the hadronic stand-alone and combined calorimeters when available, and the contributions (added quadratically except for the stand-alone ATLAS tile calorimeter) to the pion energy resolution from the stochastic term, the local constant term, and the noise are also shown, when available from published data.

D. Froidevaux, P. Sphicas Annu. Rev. Nucl. Part. Sci. 2006. 56:375–440

# ILC Calorimeters – Particle Flow Reconstruction

generated

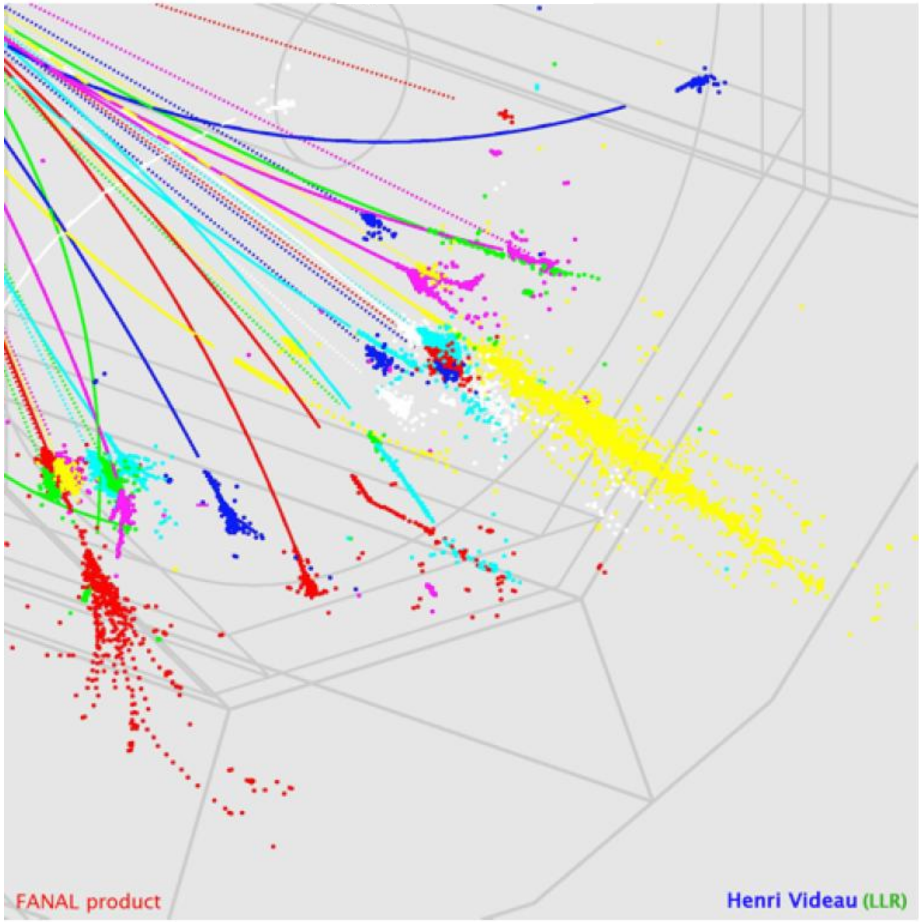


reconstructed

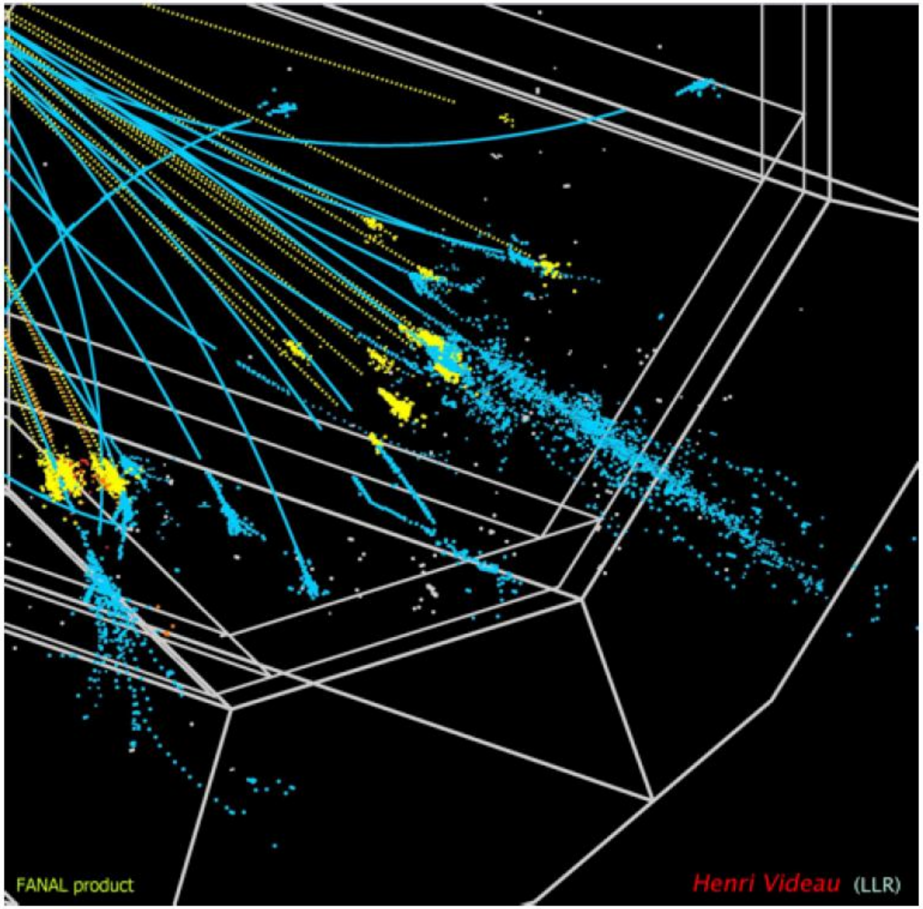

# Calorimeters for the High Luminosity LHC

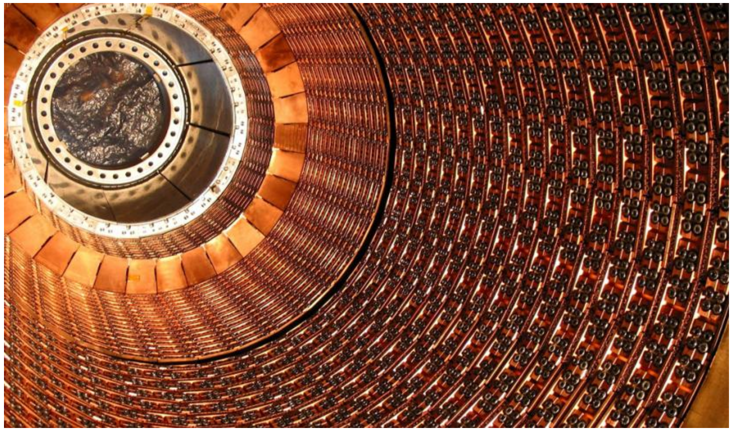

# LHC and Detector Upgrades

R. Heuer comments winter shutdown 2011-2012 (FAZ 6.10.2011):
"Die Maschine und die Detektoren brauchen dringend mal eine Pause.„
→ there are more breaks ahead....

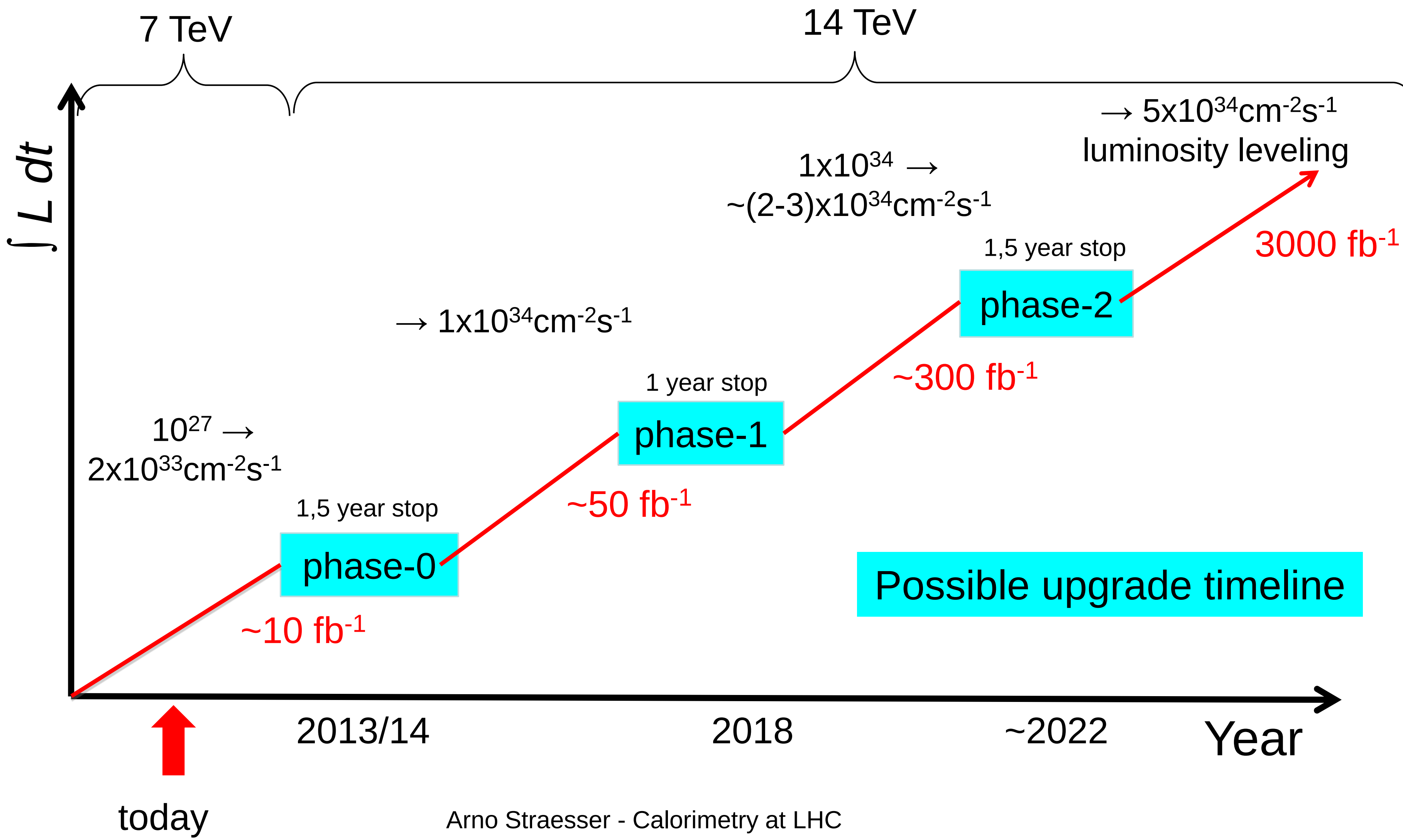

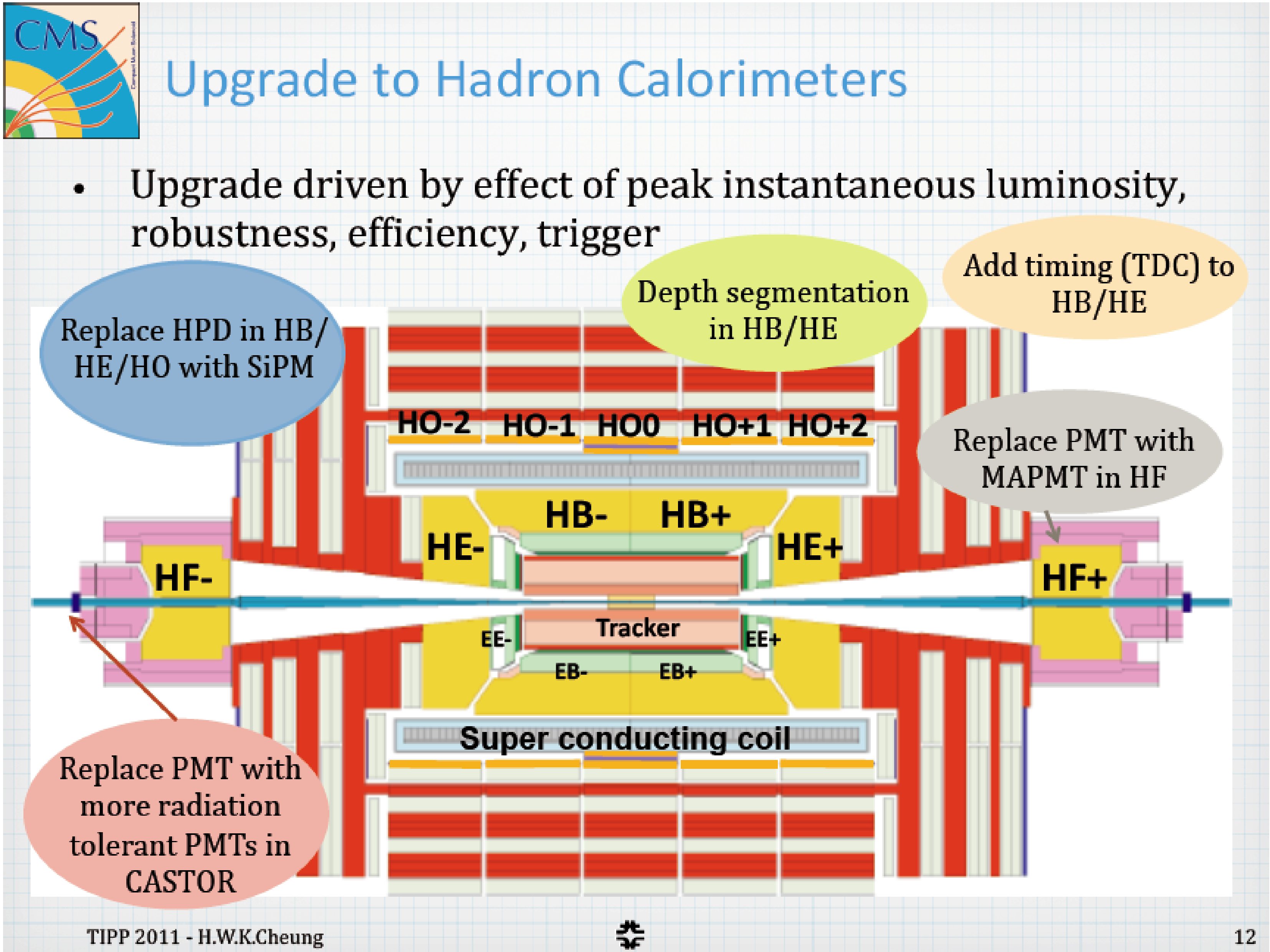
CMS
Upgrade to Hadron Calorimeters
• Upgrade driven by effect of peak instantaneous luminosity, robustness, efficiency, trigger
Replace HPD in HB/HE/HO with SiPM
Depth segmentation in HB/HE
Add timing (TDC) to HB/HE
Replace PMT with MAPMT in HF
Replace PMT with more radiation tolerant PMTs in CASTOR
HO-2
HO-1
HO0
HO+1
HO+2
HB-
HB+
HE-
HE+
HF-
HF+
EE-
EE+
Tracker
EB-
EB+
Super conducting coil
TIPP 2011 - H.W.K.Cheung
12

# CMS: Anomalous Signals in Calorimeters

- in collision data, CMS observed anomalous signals in ECAL and HCAL (now reproduced in simulation and taken into account/corrected in data analysis)

G. Tonelli ICHEP2010

## HCAL: barrel and endcap (HB,HE)

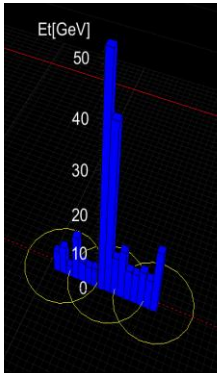


- random, low rate,
  ~ 10-20 Hz (E>20 GeV)
- caused by ion feedback, noise & discharges in Hybrid Photo Diodes (HPDs)

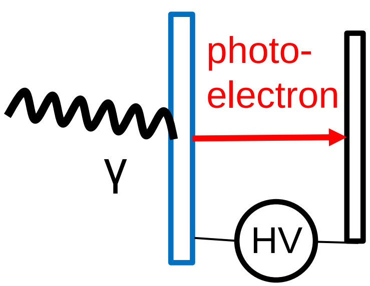


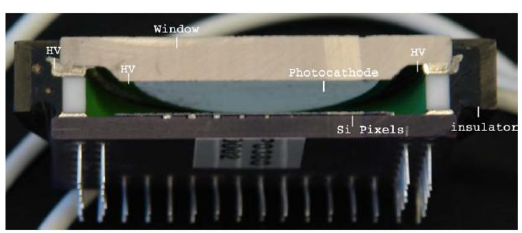


Hybrid Photo Diode

## HCAL: forward region (HF)

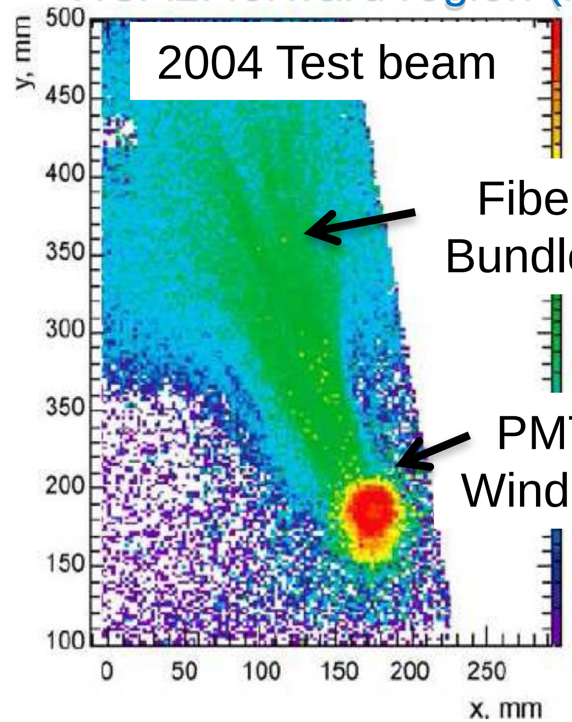


- caused by Cherenkov light by particles going through glass of Photo Multiplier Tube (PMT)

# CMS HCAL Barrel and Endcap with SiPM

- Silicon Photo Multiplier (SiPM)
- pixelated avalanche photo diodes which run in Geiger mode → very high gain
- all APDs are connected to one output
- signal is sum of all pixels

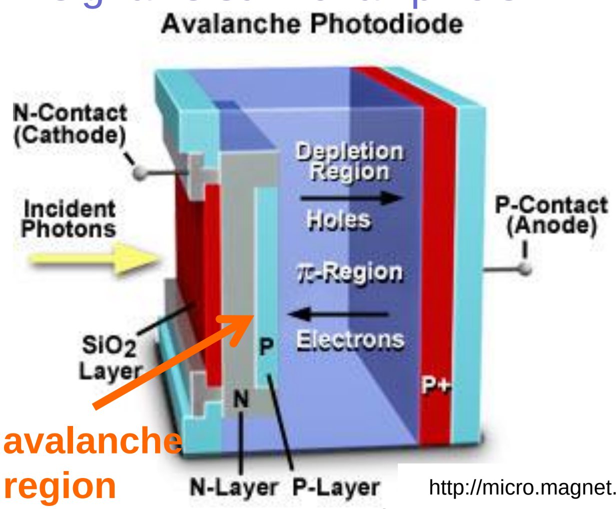


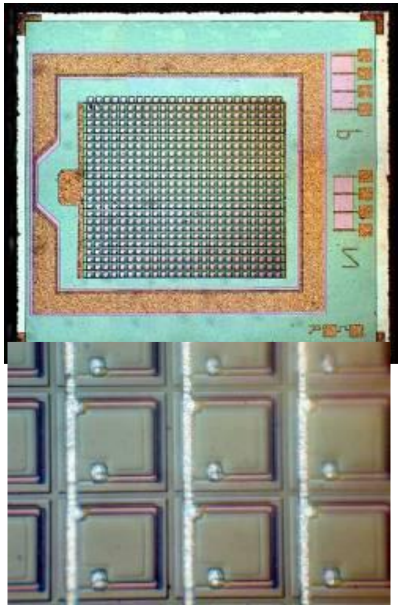

http://micro.magnet.fsu.edu
(example, not CMS design)

- array size 0.5x0.5 mm$^2$ up to 5x5 mm$^2$
- pixel size 10 µm to 100 µm

- about 30% quantum efficiency (x 2 of HPD)
- gain ≈ $10^6$ (x 500 of HPD)
- more light (40 photo-electrons/GeV), less photostatistics broadening

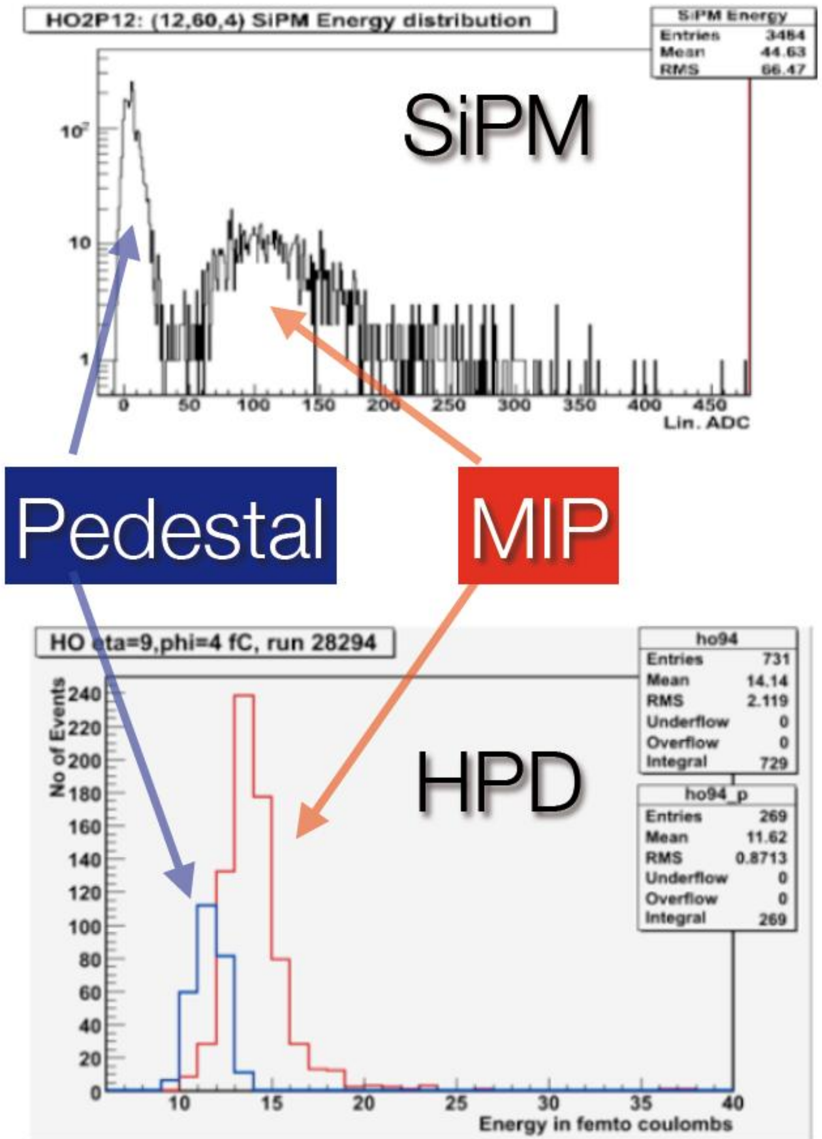


I.K. Furic ICHEP2010

# CMS HCAL barrel and endcap segmentation

- new photodetectors allow finer segmentation in HCAL depth

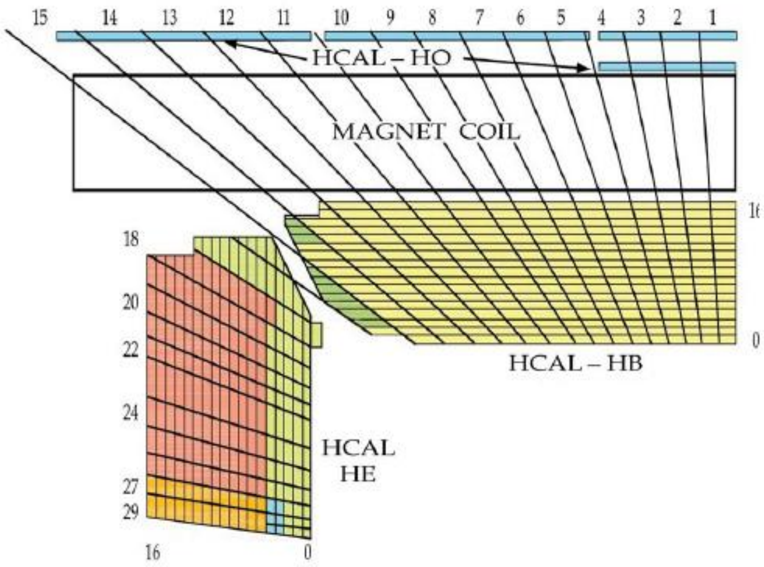


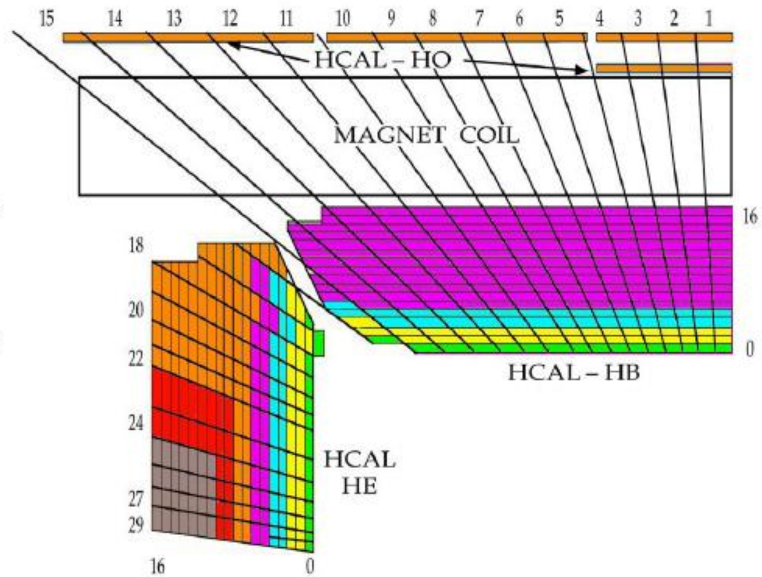


- more robust to pile-up and to damage of inner scintillator layers

- TDC measurement on inner HCAL layers yields better bunch assignment → improves lepton ID
- readout-chip is going to be replaced → read-out with higher bandwidth

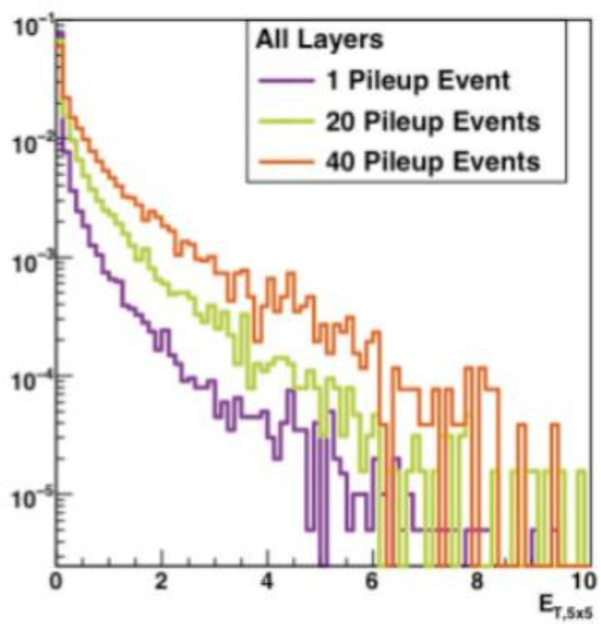


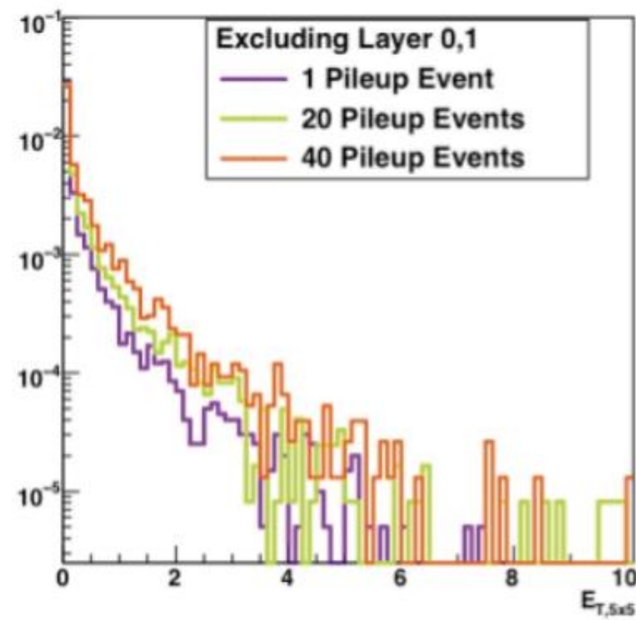

# CMS ECAL endcap crystals

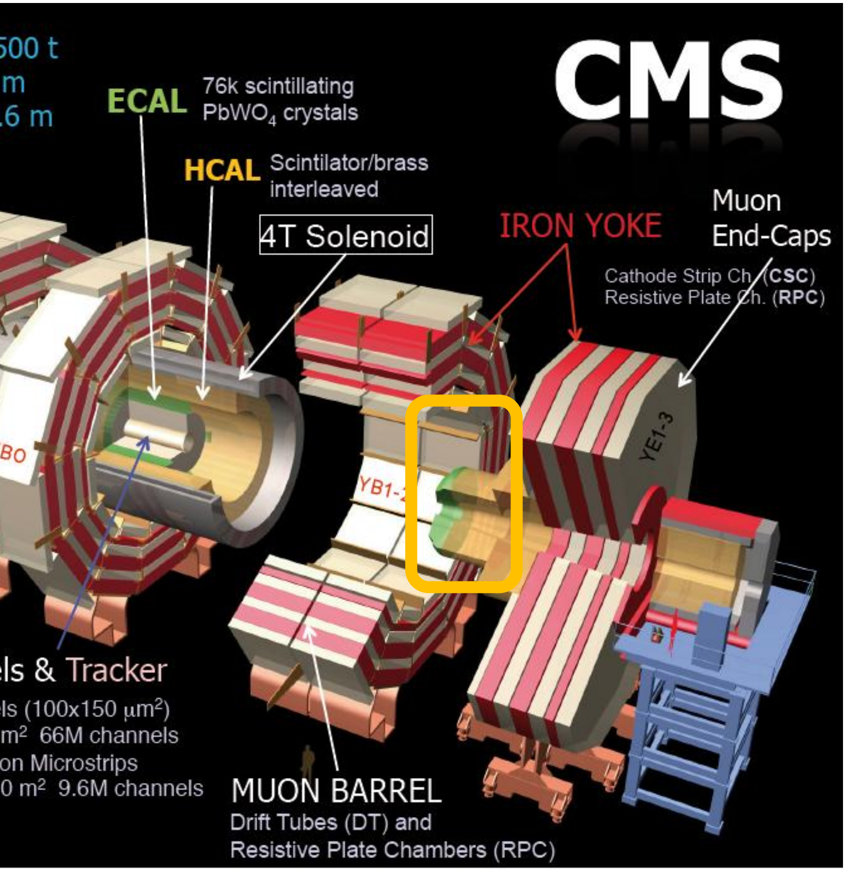



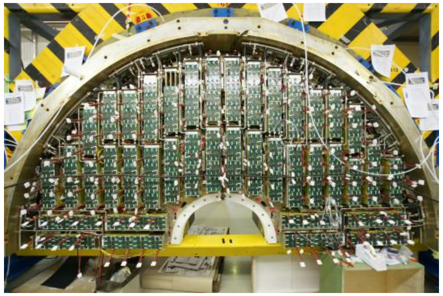

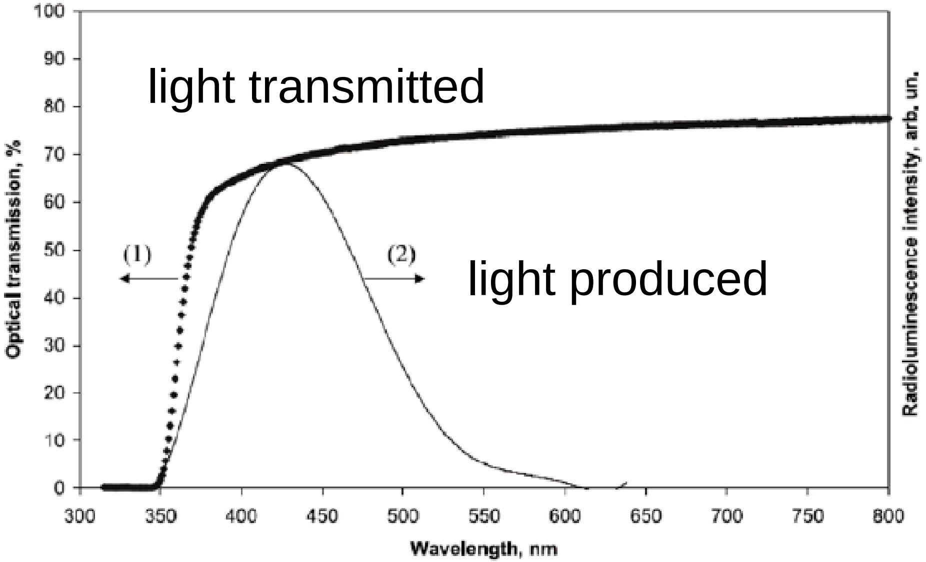


- ionisation reduces light transmission in crystals like $PbWO_4$
- absorption bands due to colour centres in crystal caused by oxygen vacancies and impurities
- scintillating light produced by hadrons and e.m. particles is not affected
- concerns when exposed to extremely high radiation dose in mixed particle beams

# CMS ECAL endcap crystals

hep-ph/0511012

- reduced light transmission is observed in test beam
- not caused by ionising radiation damage but cumulative hadron-specific damage

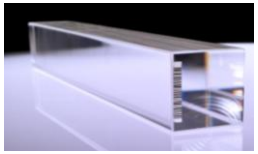

- expected hadron fluences in ECAL barrel (endcap) after 10 yrs of LHC: $10^{12}$($10^{14}$) hadrons/cm$^2$
- proton and photon induced damage measured with photo-spectrometer:

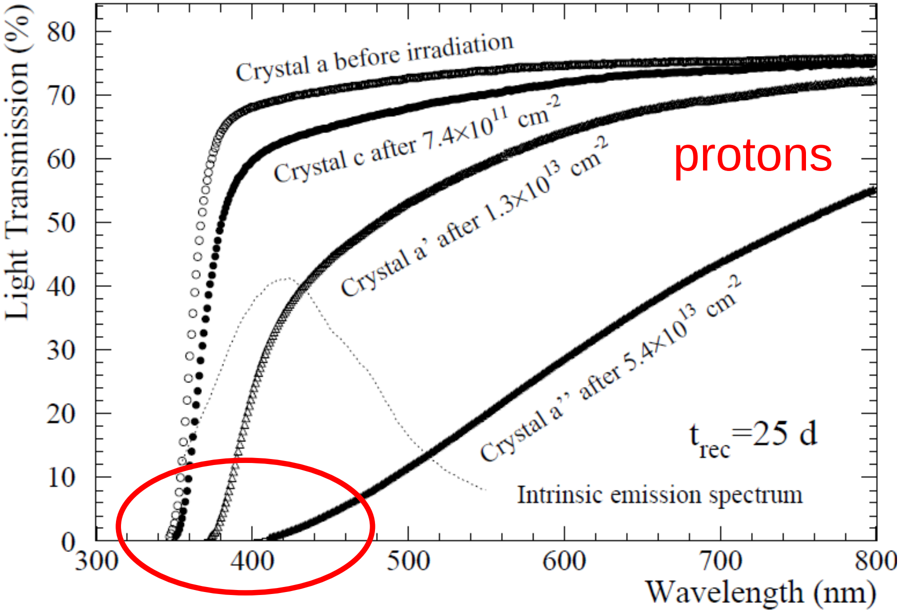


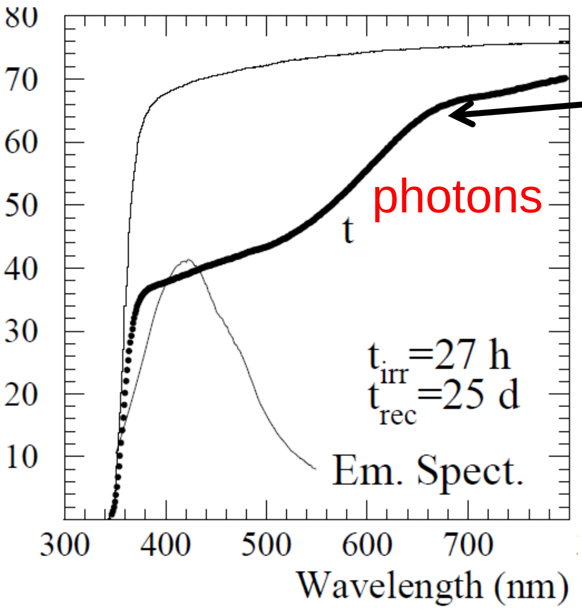


at 1 kGy/h ~ $10^{12}$ p/cm$^2$/h

cumulative damage by hadron fluence: band-edge shift

- loss in light transmission could be monitored by external light injection → crystal calibration
- replacement of ECAL endcap crystals is under discussion (Phase-2)

# The ATLAS Calorimeter Electronics

- 4 high granularity LAr calorimeters
- 182486 readout channels

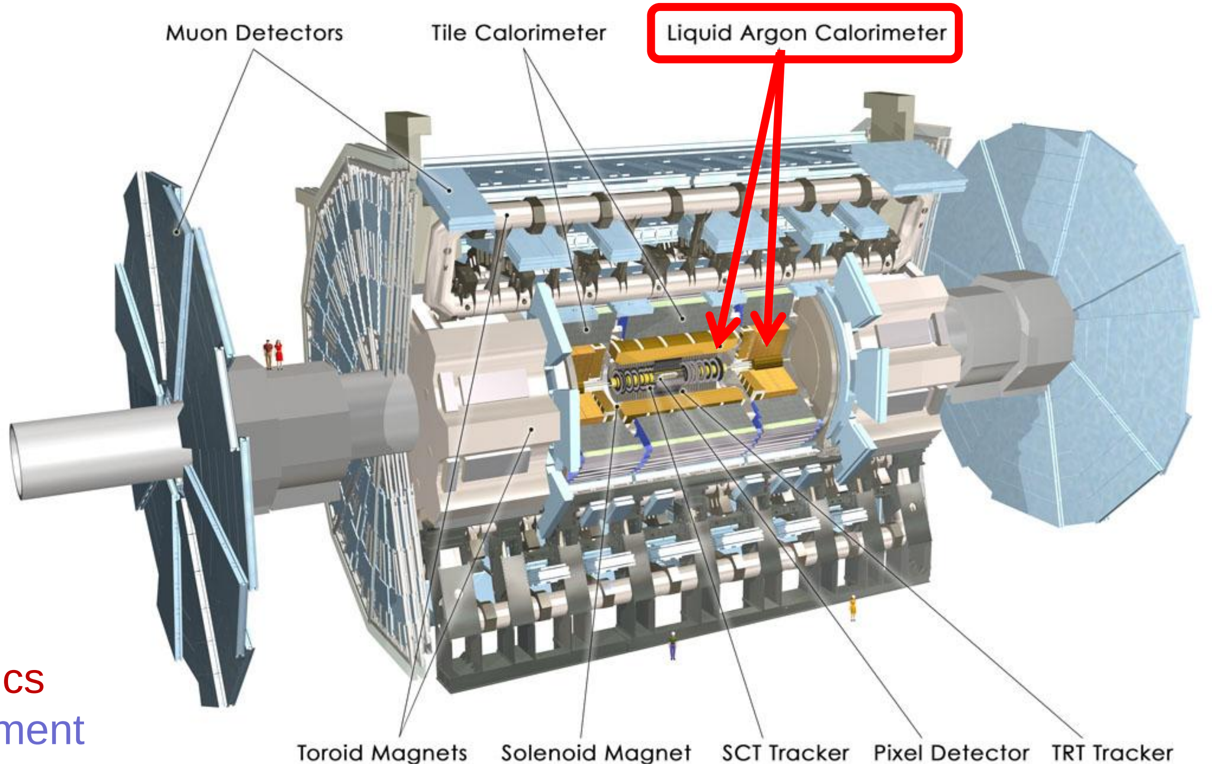


- front-end and trigger-sum electronics
  → on-detector in radiation environment
  → new trigger readout with higher granularity for improved trigger (phase-1)
  → new front-end electronics because of radiation, aging, trigger improvement (phase-2)

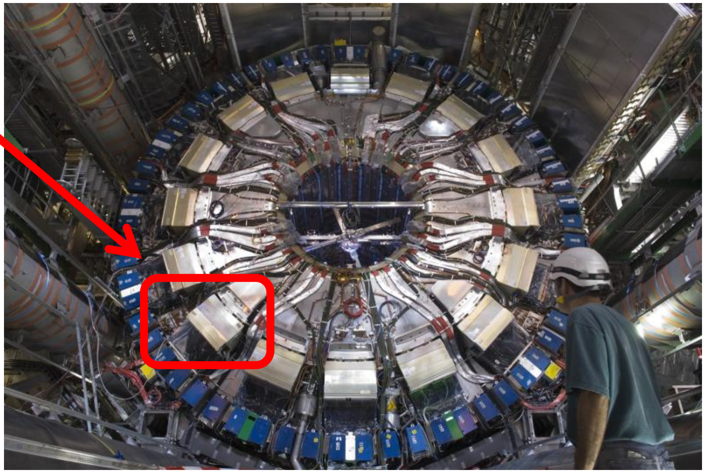

- back-end electronics and more trigger logic
  → shielded counting room
  → new electronics because of trigger improvement and aging(phase 1+2)

# ATLAS Current FCal

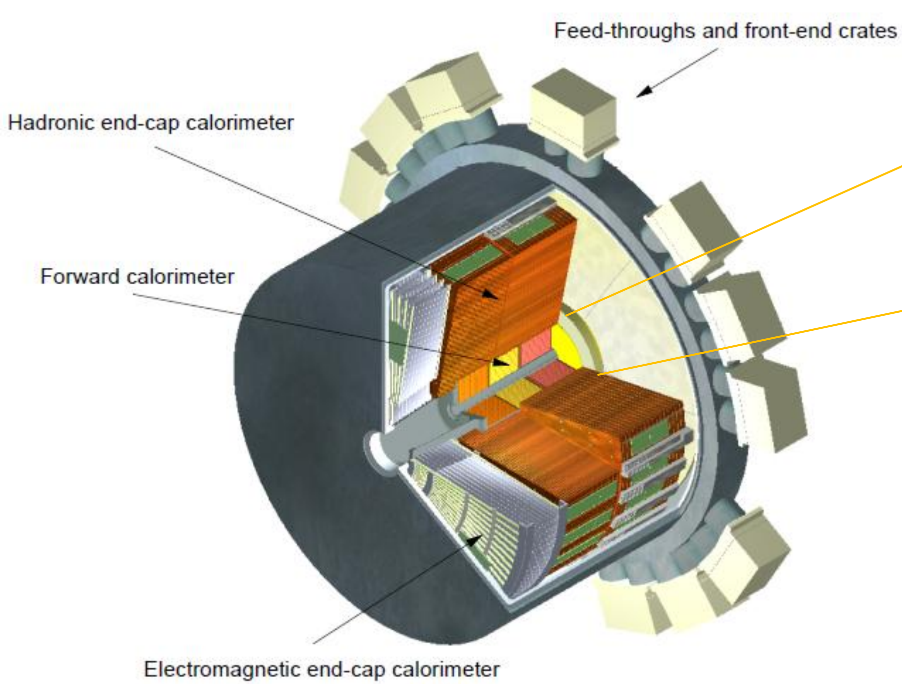


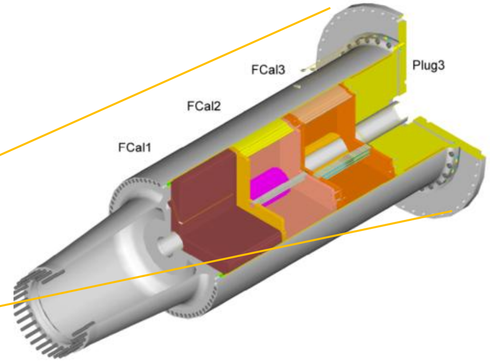


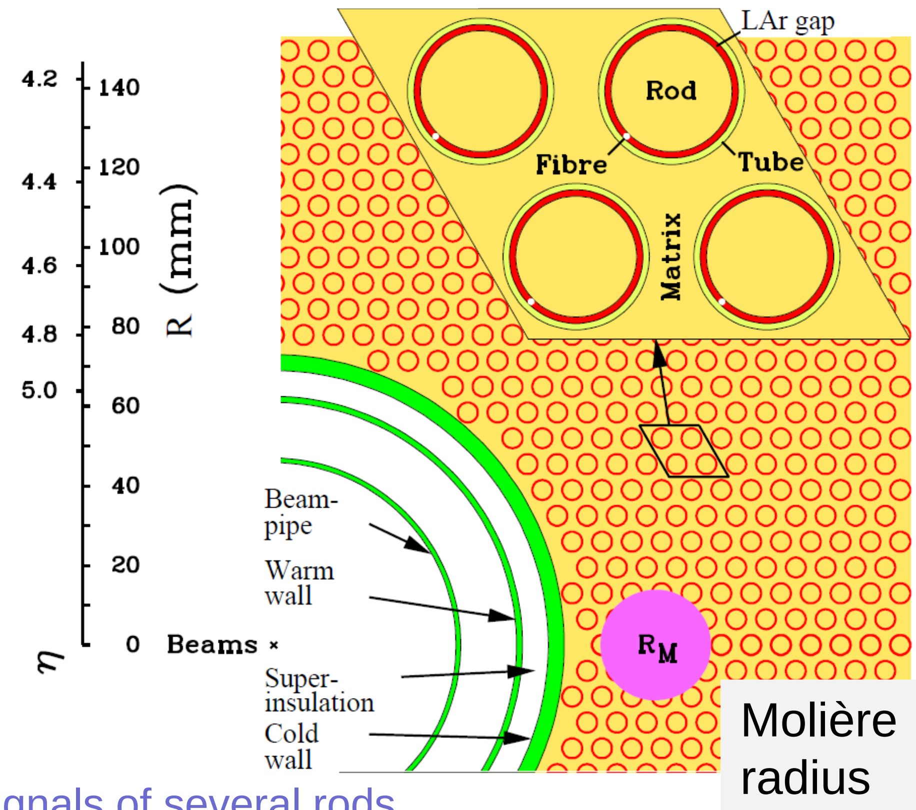


- 3 sections: FCal 1/2/3
- FCal1: Cu absorber, LAr active material
  → e.m. showers ($X_0$ = 27.6 cm, λ = 2.66 cm)
- FCal2/3: W+LAr → hadronic showers
  ($X_0$ ≈ 90 cm, λ ≈ 3.6 cm)
- detector concept:
  - absorber matrix with hollow tubes
  - inside: precision metal rod fixed with fibre
  - ionisation in LAr gap, read-out combines signals of several rods
  - gap sizes: 269 μm (FCal1) 376/508 μm (FCal2/3)

# Limitations of Current FCal

- current FCal1 will work properly up to luminosities of $1x10^{34}$ $cm^{-2}s^{-1}$
- the FCal1 will however not work efficiently above $3x10^{34}$ $cm^{-2}s^{-1}$
- reasons:
  - positive Ar ion buildup leads to field distortion and to signal loss
  - high HV currents lead to voltage drop
  - heating of LAr and boiling (only at very high luminosities)

- all effects related to:
  - particle rate ~ peak luminosity (not integrated luminosity)

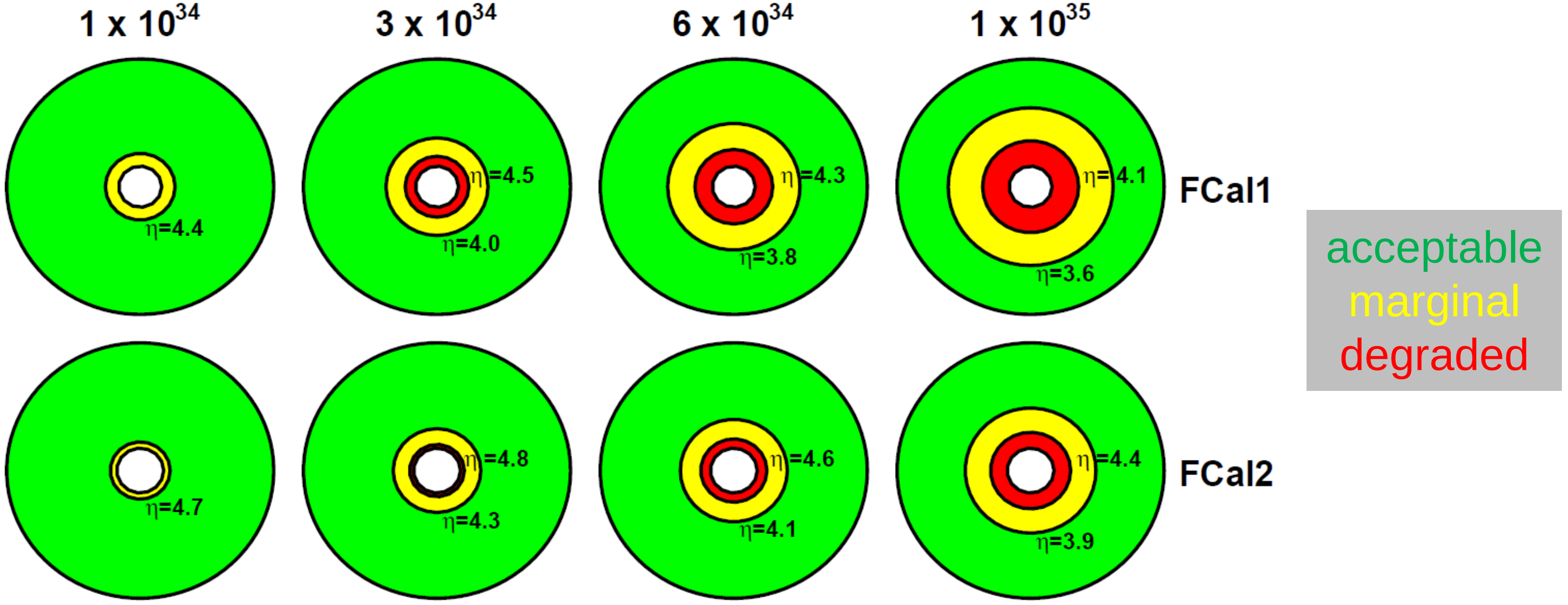

# Limitations of Current FCal

- LAr heating/boiling can possibly be cured with additional $LN_2$ cooling loops

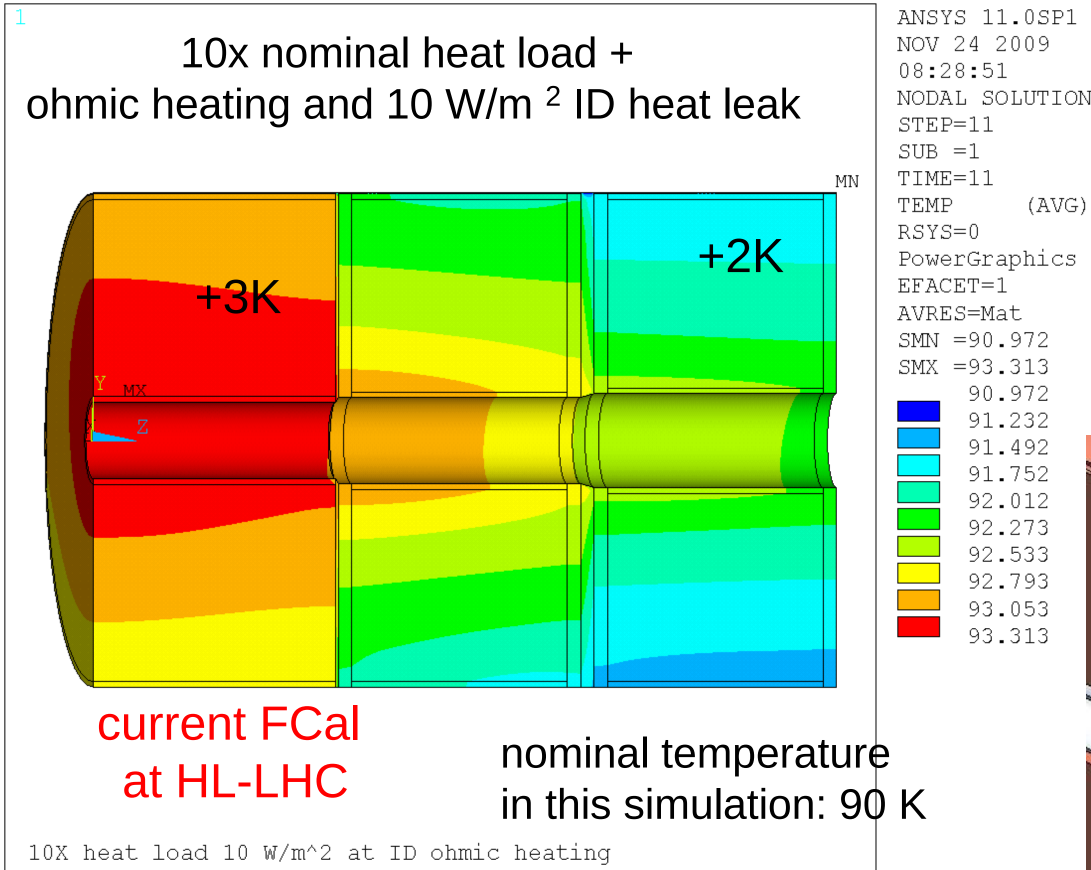


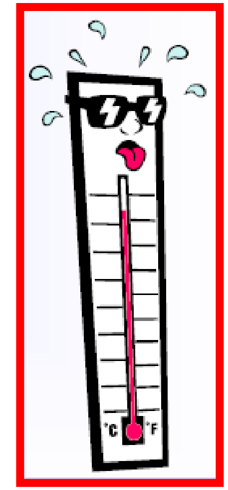

$LN_2$ cooling pipes

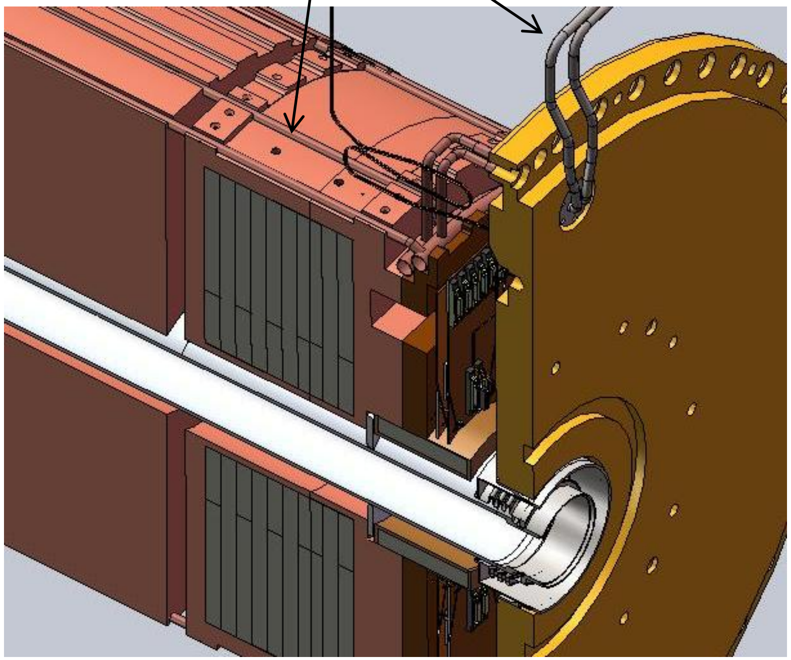

- $LN_2$ cooling can remove a 10x LHC heat load (562 W on 3.787 $m^2$ surface) using a flow of 0.0028 kg/s at 0.070 m/s

# Signal degradation in LAr gap

- critical ionisation rate: rate of newly created Ar+ ions equal to rate in which ions are removed from the gap
- r = rate relative to critical rate
- relative of LAr+ e- recombination rate w
  - w=0 no recombinations
  - $w \rightarrow \infty$ recombination removes practically all Ar+ e- pairs
- signal is obtained from fast-moving e- (Ar+ are slow)

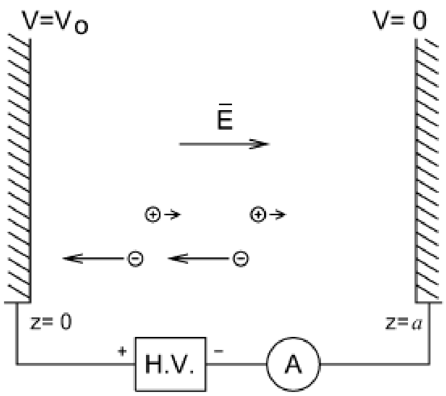


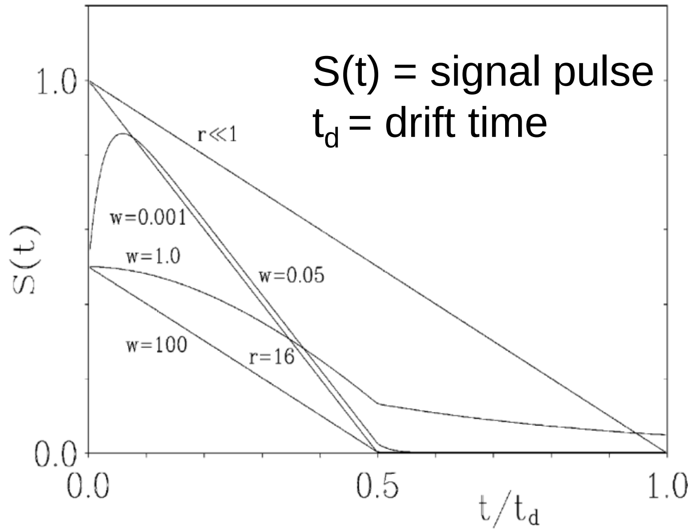


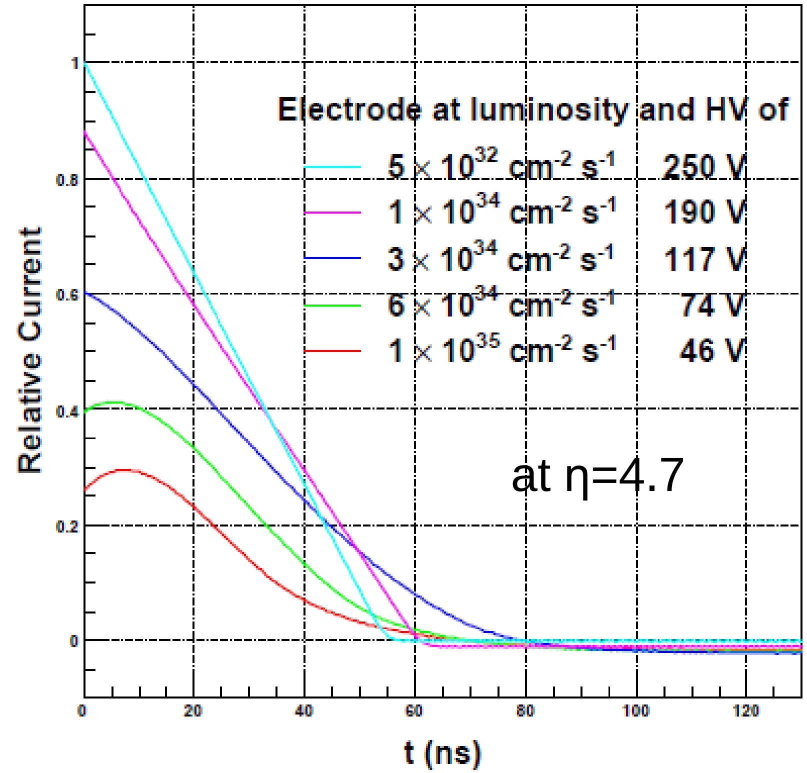


- at high luminosity
  - not all Ar+ are removed from gap → ion build-up
  - recombination rate rises → slow-rising pulse
  - although HV resistors have high value
    → voltage drop over LAr gap
- amplitude no more proportional to energy deposit

# ATLAS sFCal for Phase-2

- solution 1: smaller LAr gaps reduce ion build-up effects and HV drop
- build new sFCal (Cu/LAr) calorimeter with 100 μm gaps instead of 250 μm to replace FCal1

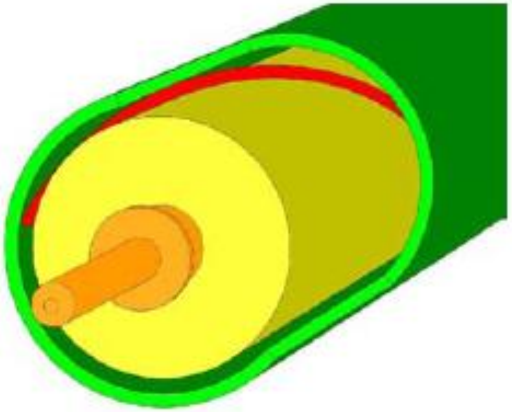

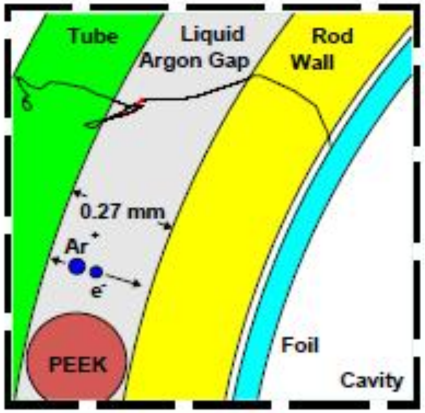


- test beam measurement of pulse shapes in Protvino/Russia with a high-intensity proton beam

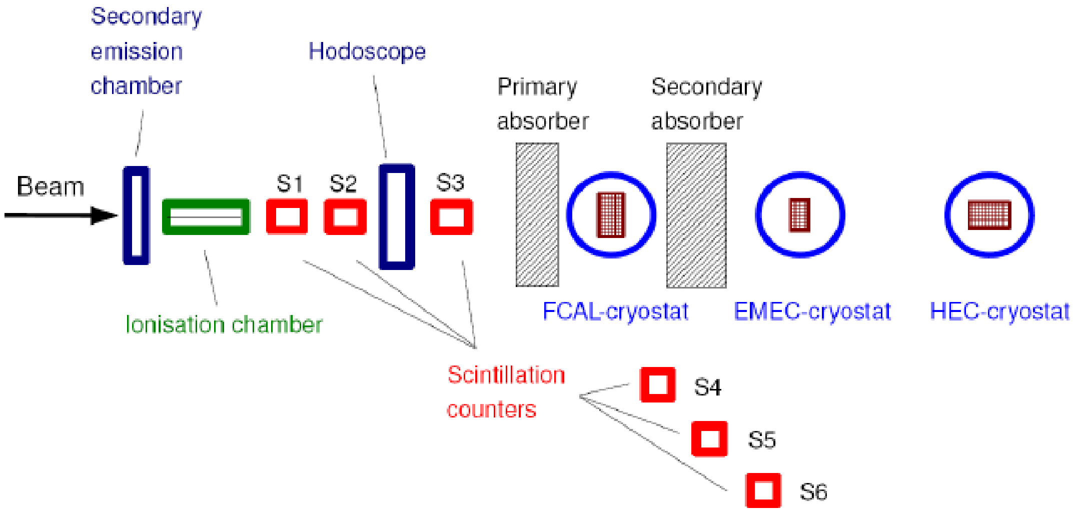


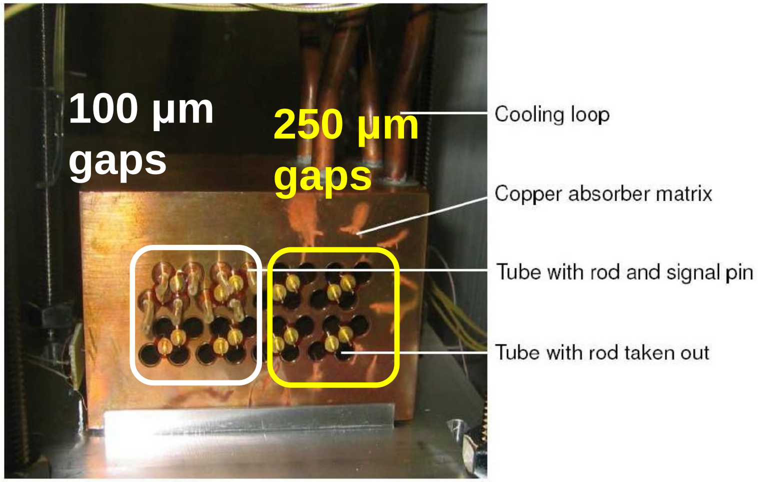

# ATLAS MiniFCal

- new sFCal would require an opening of the endcap cryostat
  - very difficult and risky operation
    → FCal, electromagnetic and hadronic endcap calorimeters are in the same cryostat
  - components will be activated → requires additional safety measures during module extraction
  - only performed if new front-end electronics for the hadronic endcap calorimeter is needed

- solution 2: new MiniFCal in front of current FCal → in front of endcap cryostat

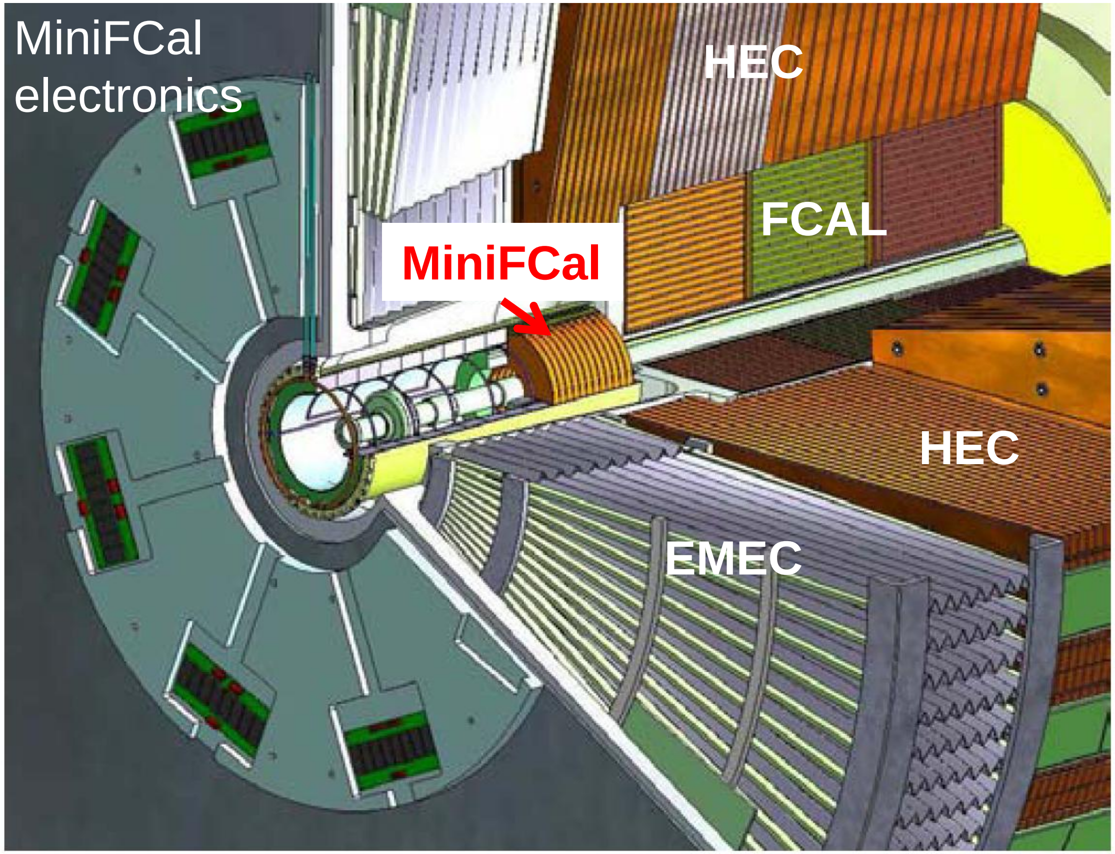

# ATLAS MiniFCal for Phase-2

- technology: Cu absorbers and diamond detector disks
- neutron flux ~5 x $10^{17}$ n/cm$^2$ (10 yr HL-LHC): copper 3x higher absorption rate than tungsten

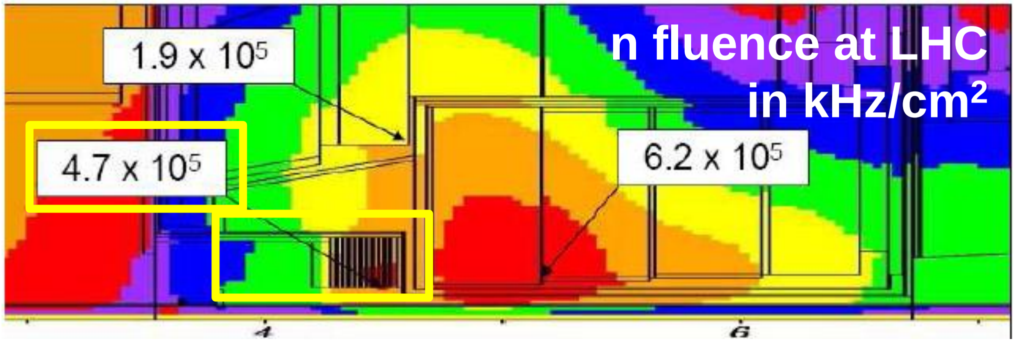


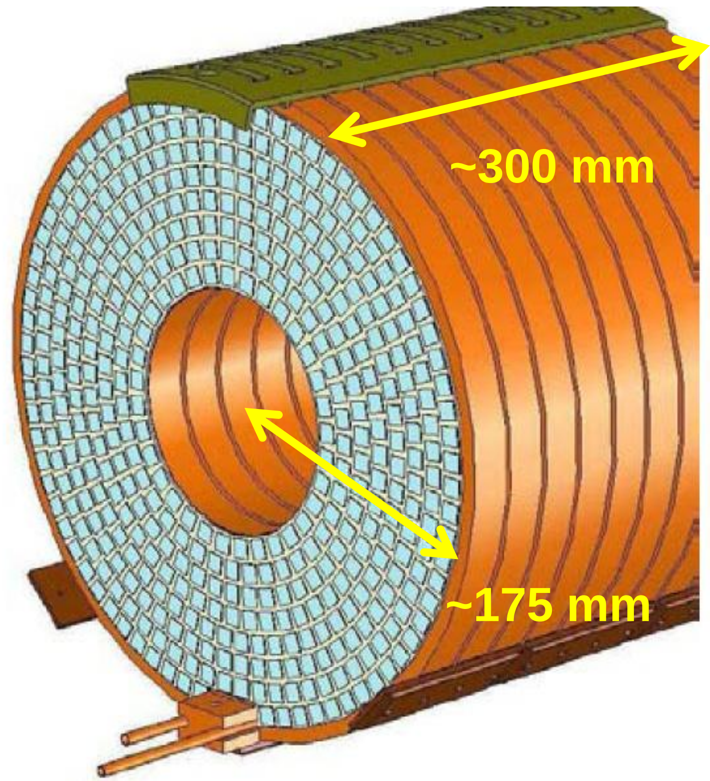


- 12 Cu disks and 11 detector planes
- 18.8 radiation lengths
- sampling fraction 0.005

- ~5000 diamond pixels 1cm x 1cm

- absorption in Cu disks reduces energy deposit in FCal1 by 45%

- voltage drop in FCal less than 50 V for radius>11 cm
  → only 3% of FCal affected by HV-drop

| MeV/100 evts | No Mini-FCal | Baseline Mini-FCal |
|---|---|---|
| Mini-FCal | - | $1.48 \times 10^7$ |
| FCal1 | $1.92 \times 10^7$ | $1.06 \times 10^7$ |
| FCal2 | $5.97 \times 10^6$ | $3.09 \times 10^6$ |
| FCal3 | $1.35 \times 10^6$ | $8.53 \times 10^5$ |

# ATLAS MiniFCal

- simulated energy response and resolution to single electrons of 200 MeV:

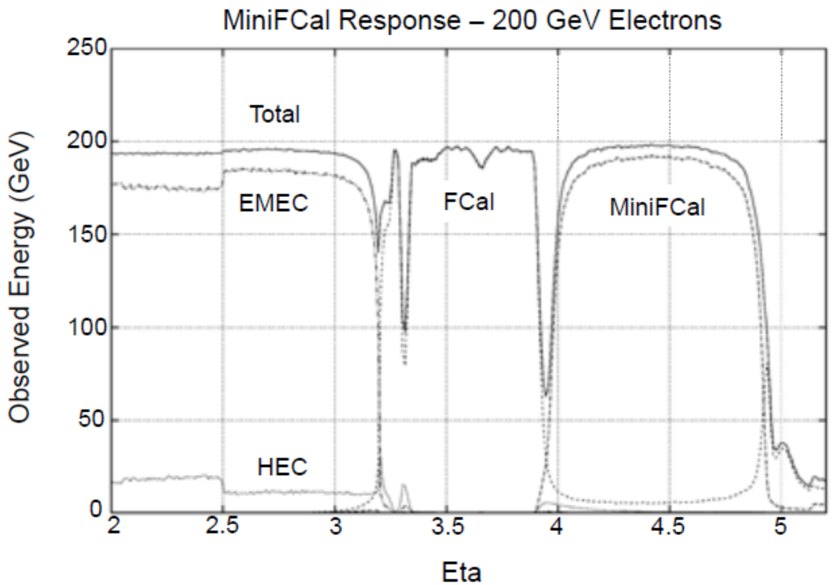


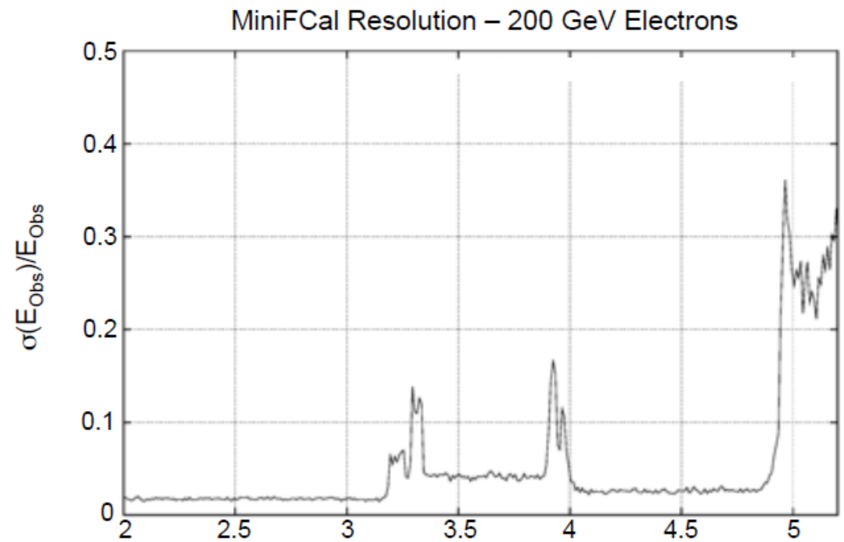


- resolution typically <5% in MiniFCal region and better than ~30% down to |η|~5.3

- diamond-Cu sampling device is difficult to calibrate: strong dependence on particle fluence

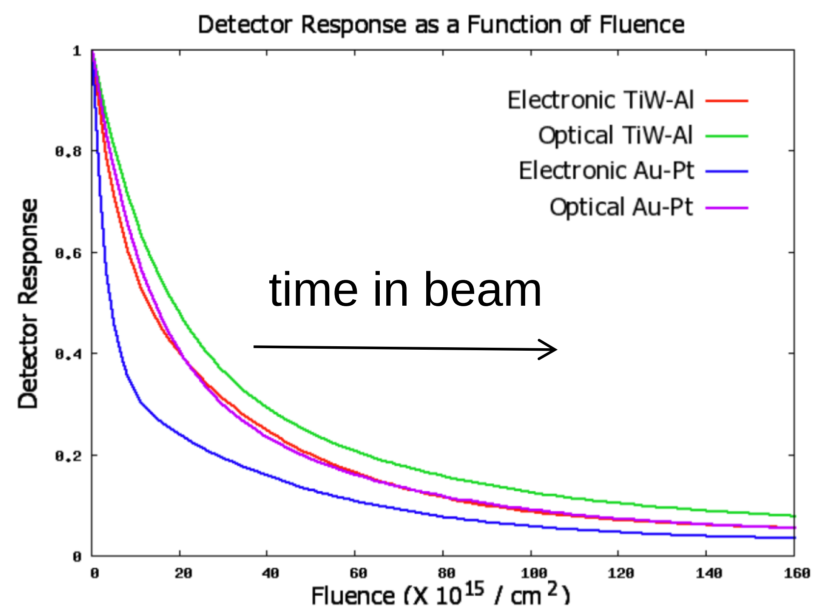

# How to find out what is the best solution?

- detector simulations
  - rough estimate: Monte Carlo generator level with acceptance cuts

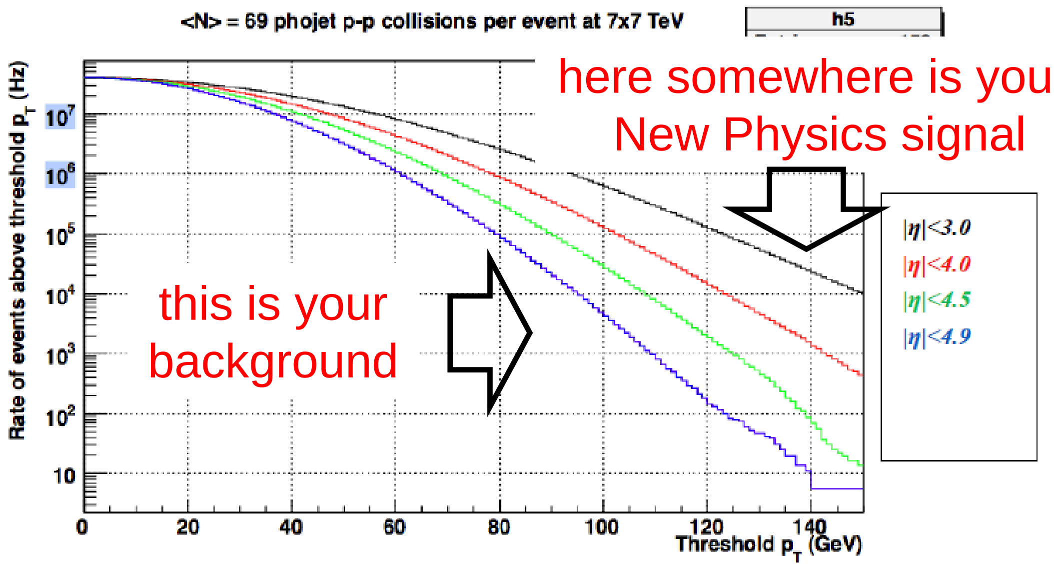


example:
missing $E_T$ tails if detector acceptance is reduced

  - best with realistic geometry, all physics effects, detector response functions, calibration, ...

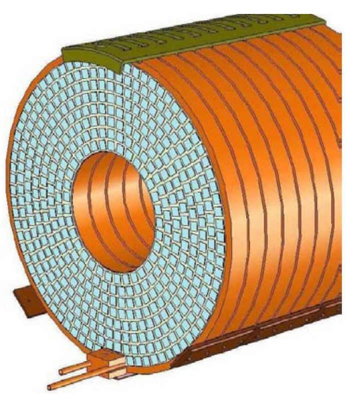

engineering drawing
→ simulation tool

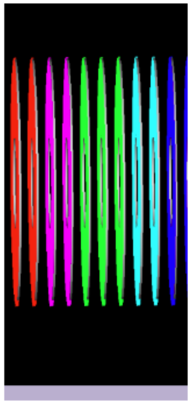

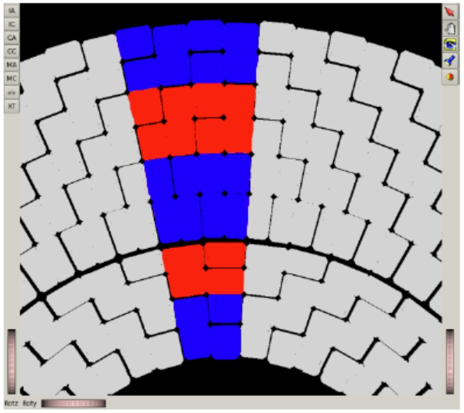

# Simulation Framework Geant4

key tasks:

- tracking, and geometrical propagation including magnetic field
- modelling of physics interactions
- visualization, persistency

and enable you to describe your setup:

- detector geometry
- radiation source
- details of sensitive regions

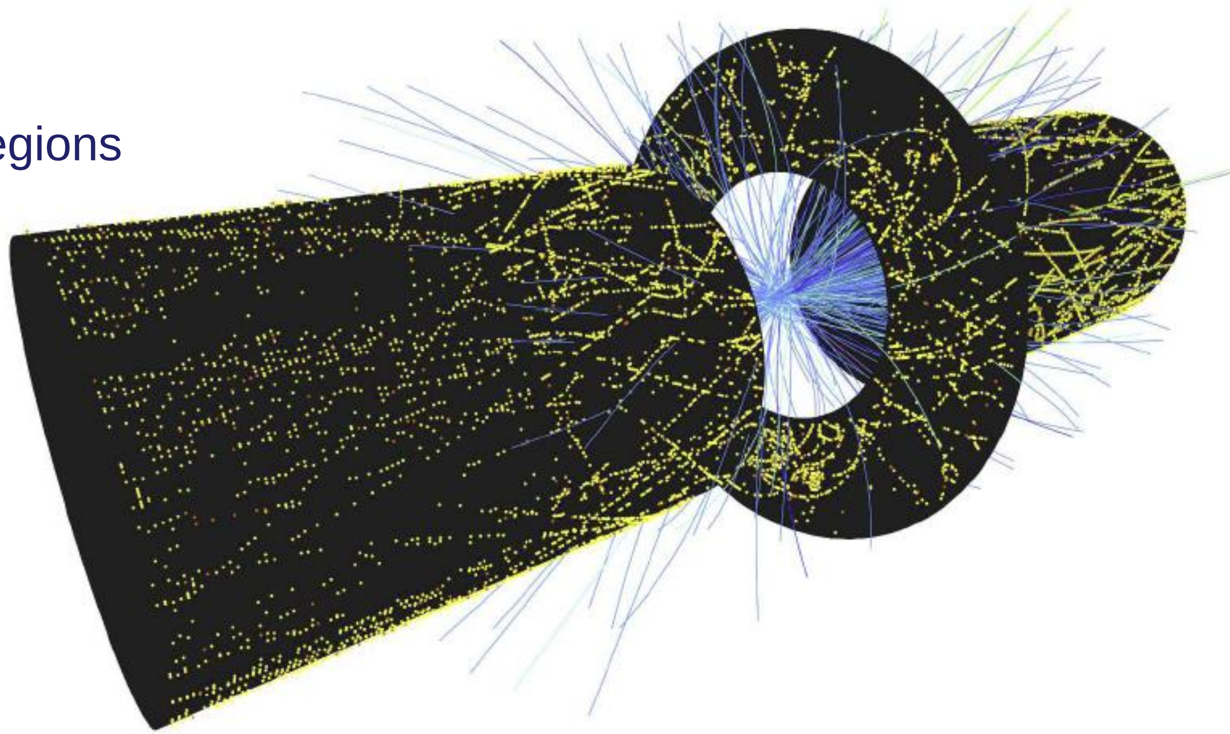

The ATLAS Simulation Infrastructure
arXiv:1005.4568

**Fig. 7.** A Higgs boson decaying into four muons, with only the inner detector tracks and hits in the TRT being displayed by VP1.

# Summary

- LHC Calorimeters – „classic“ calorimeters adapted to hadron machine conditions
- ILC Calorimeters – reconstruction of e.m. and hadronic shower details – particle flow
- non radiation-hard technologies will see problems in High Luminosity LHC phase
- new solutions are being worked on – a project of the next 10 years (and maybe more...)

# More information

# The path to the future – part 2

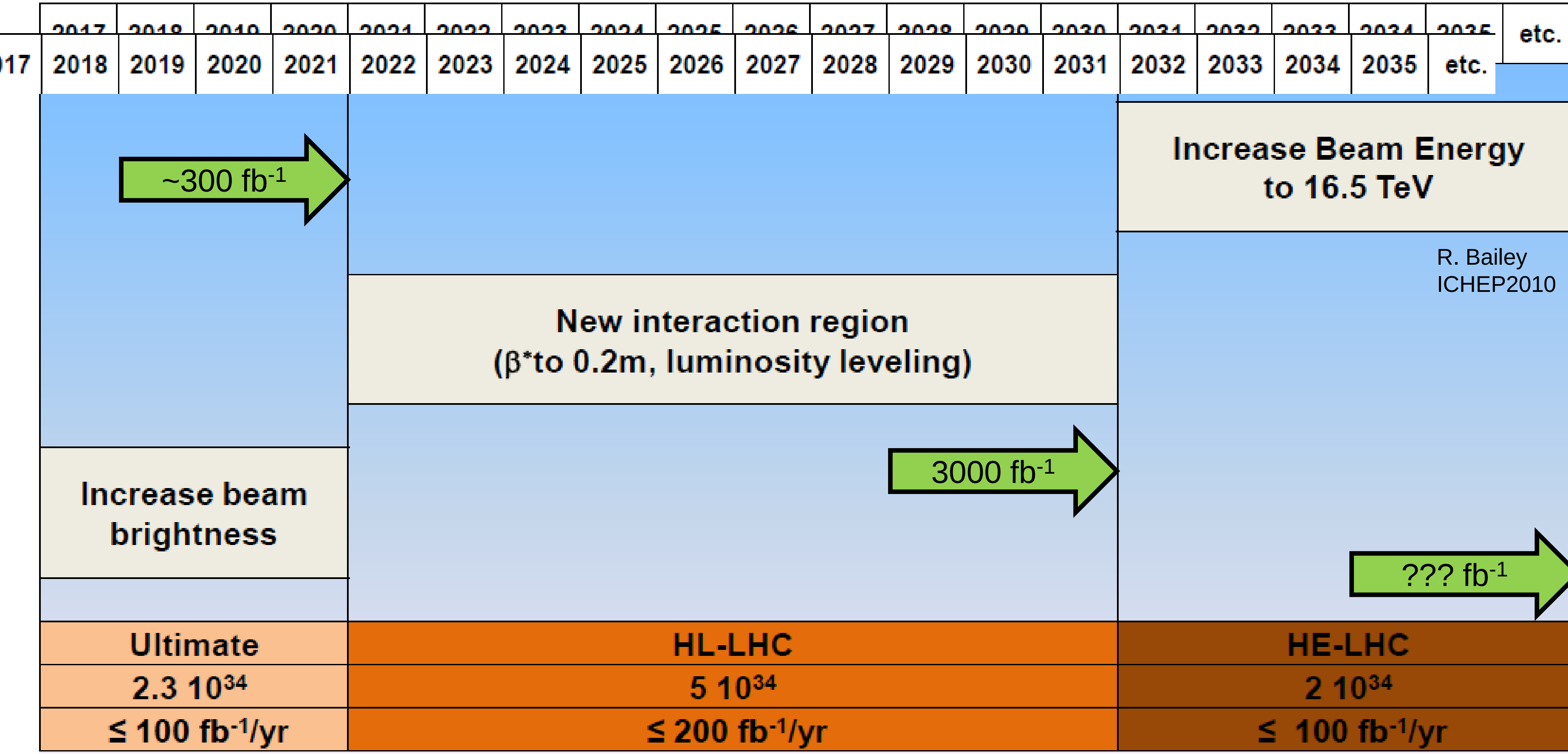


- higher intensity requires upgrades of CERN accelerator complex (Linac 4, LP-SPL/PS2, PSB+)
- small β* and modification of the interaction region, e.g. crab cavities
- luminosity leveling: start a fill with non-max luminosity → avoid exponential lumi decrease → optimize total lumi yield

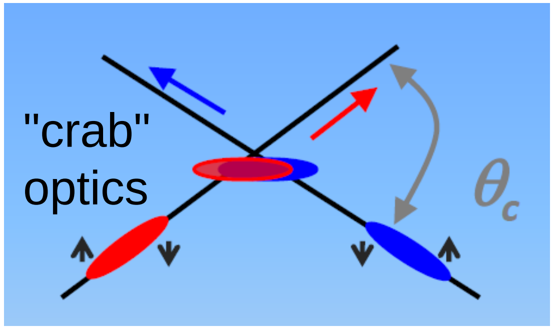

# Luminosity Leveling

- luminosity evolution today in one fill:

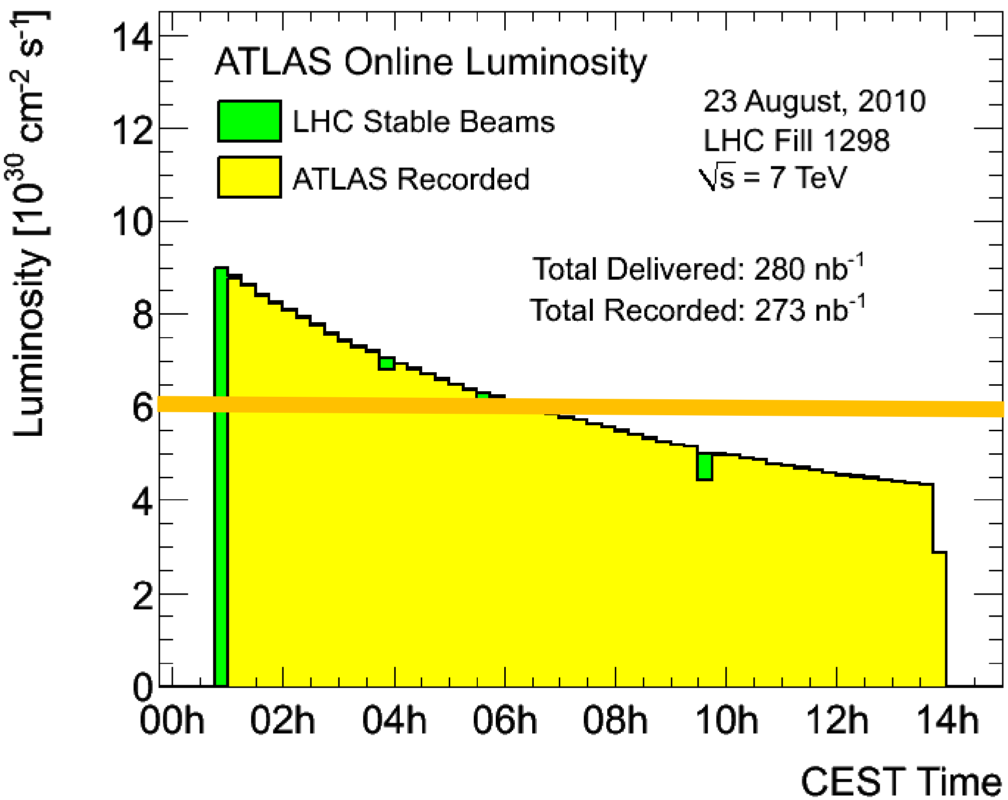


- possible luminosity evolution at HL-LHC:

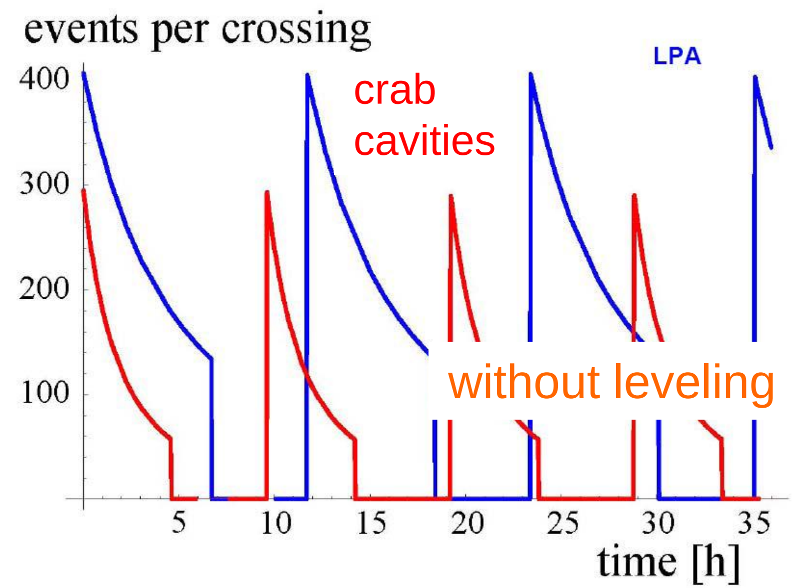


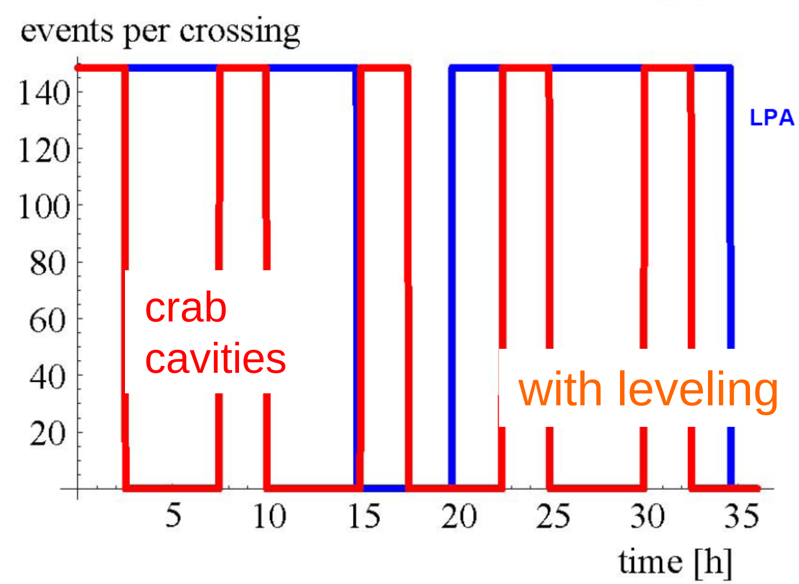


- luminosity leveling:
  - reduced and constant pile-up rate during one fill

- Tile Calorimeter: Fe/Scintillator

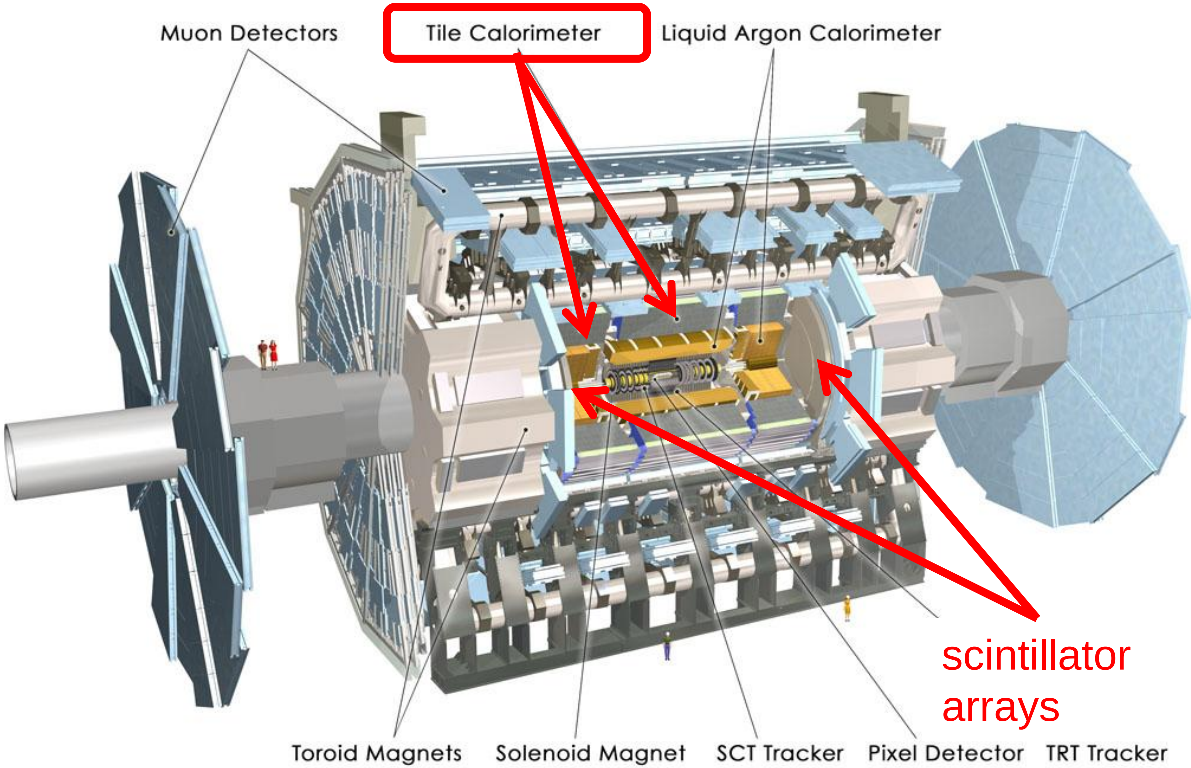


- Tile Calorimeter pgrade plans:
  - electronics, connectivity, cooling is arranged in "drawers" → replace with newly designed modules
  - replacement of gap and cryostat scintillators (possibly MicrOmegas)

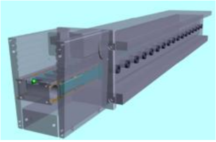

- new readout-electronics (same arguments as for LAr read-out)
  - higher radiation tolerance, normal ageing of components
  - improved trigger capabilities → higher granularity